AD-A144 253 DECISION RULES APPLIED TO SPREAD SPECTRUM SIGNAL DETECTION(U) NEW JERSEY INST OF TECH NEWARK R J KIM ET AL. JUL 84 CECOM-TR-84-3 DAAG07-82-K-J156 1/1

UNCLASSIFIED F/G 9/3 NL

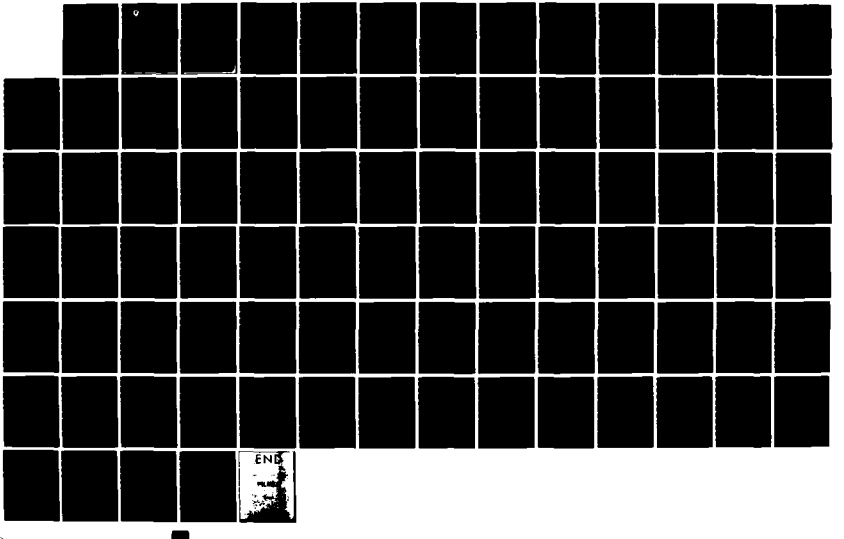

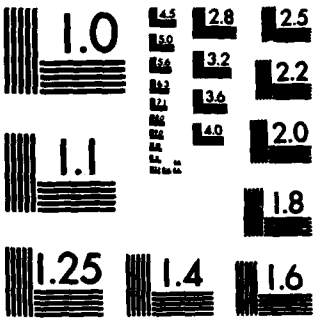

RESEARCH AND DEVELOPMENT TECHNICAL REPORT

CECOM-TR-84-3

DECISION RULES APPLIED TO SPREAD SPECTRUM SIGNAL DETECTION

RICHARD J. KIM
SOLOMON ROSENSTARK
JOSEPH FRANK
CENTER FOR SYSTEMS ENGINEERING & INTEGRATION

JULY 1984

CECOM
U S ARMY COMMUNICATIONS-ELECTRONICS COMMAND
FORT MONMOUTH, NEW JERSEY 07703

NOTICE

Disclaimer

The citation of trade names and names of manufacturers in this report is not to be construed as official Government endorsement or approval of commercial products or services referenced herein.

Disposition

[illegible] Destroy this report when no longer needed. Do not

UNCLASSIFIED

SECURITY CLASSIFICATION OF THIS PAGE (When Data Entered)

REPORT DOCUMENTATION PAGE	READ INSTRUCTIONS BEFORE COMPLETING FORM
1. REPORT NUMBER: CECOM-TR-84-3	2. GOVT ACCESSION NO.: AD-A144253	3. RECIPIENT'S CATALOG NUMBER
4. TITLE (and Subtitle): DECISION RULES APPLIED TO SPREAD SPECTRUM SIGNAL DETECTION	5. TYPE OF REPORT & PERIOD COVERED: Technical Report June 1982 - June 1983
	6. PERFORMING ORG. REPORT NUMBER
7. AUTHOR(s): Richard J. Kim, Solomon Rosenstark, Joseph Frank	8. CONTRACT OR GRANT NUMBER(s): DAAB07-82-K-J156
9. PERFORMING ORGANIZATION NAME AND ADDRESS: US Army Communications-Electronics Command, Center for Systems Engineering & Integration (CENSEI) ATTN: DRSEL-SEI-F, Fort Monmouth, NJ 07703	10. PROGRAM ELEMENT, PROJECT, TASK AREA & WORK UNIT NUMBERS
11. CONTROLLING OFFICE NAME AND ADDRESS: Same as above	12. REPORT DATE: July 1984
	13. NUMBER OF PAGES: 84
14. MONITORING AGENCY NAME & ADDRESS(if different from Controlling Office)	15. SECURITY CLASS. (of this report): UNCLASSIFIED
	15a. DECLASSIFICATION/DOWNGRADING SCHEDULE

16. DISTRIBUTION STATEMENT (of this Report)

Approved for public release; distribution is unlimited.

17. DISTRIBUTION STATEMENT (of the abstract entered in Block 20, if different from Report)

18. SUPPLEMENTARY NOTES

19. KEY WORDS (Continue on reverse side if necessary and identify by block number)

Chips, Symbols, Words, Detector, Correlator, Decoder

Sub E Sub S

20. ABSTRACT (Continue on reverse side if necessary and identify by block number)

Decision rules for detection of spread spectrum signals were investigated. For each decision rule, error and erasure probabilities were analyzed. The obtained data was used to plot P_E vs. P_e for constant signal-to-noise ratio (SNR). With the use of the probability-of-a-word-error curves the optimum threshold setting was found for a given SNR.

(see reverse)

DD FORM 1 JAN 73 1473 EDITION OF 1 NOV 65 IS OBSOLETE

UNCLASSIFIED

SECURITY CLASSIFICATION OF THIS PAGE (When Data Entered)

20. ABSTRACT (contd)

Orthogonal signalling (FSK) and antipodal signalling (PSK) were considered for modulating the chips. When the P_B vs. P_e plots for FSK and PSK were compared, PSK performed better than FSK by a ratio of 6 dB.

Finally, analog and digital correlation of the received signals was investigated. Compared to the performance of analog correlation, the system performance for digital correlation was worse by less than 1 dB.

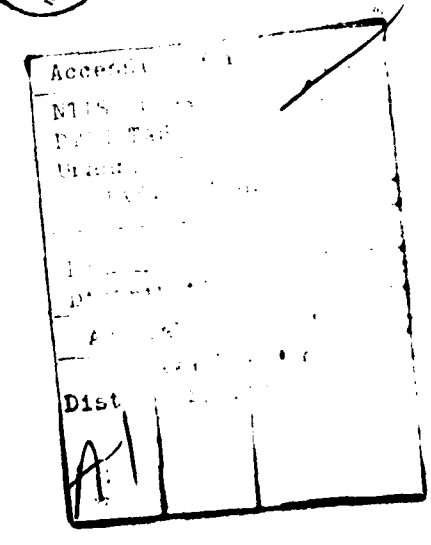

TABLE OF CONTENTS

LIST OF FIGURES

CHAPTER 1

INTRODUCTION

This report is the result of CENSEI's basic research work on critical issues concerning system engineering and integration of spread spectrum systems, in concert with applications of distributed systems architectures, to provide information distribution for C^2 information management systems operating in a communications-bounded environment. In a communications-bounded environment, subscribers on a given network are transmitting at maximum subscriber capacity. Network capacity is not the simple sum of subscriber capacities. Rather, it can be a complex function of the number of subscribers, their topological distribution, and their offered traffic load. The RF resource, however, is limited, and saturation, which translates to self-jamming, will result as more subscribers are operating, or as more capacity is allocated and utilized by each subscriber. The long term goal is to derive a meaningful portrayal of performance degradation due to self-jamming in spread spectrum system candidates for the Army's survivable C^3 network. Such a portrayal will then be used by the Army system engineers to ensure that network capacity is adequate for given user applications. Initially, performance degradation was studied for hybrid direct-sequence/frequency-hop systems. In the course of this study, it became apparent that performance degradation was also a function of the receiver decision logic, which is the subject of this report.

The spread spectrum communications system which was studied uses an alphabet of 32 symbols to communicate messages. A symbol is represented by a

sequence of 32 chips. (A chip is a binary (+1,-1) digit which takes on a value of either +1 or -1.) A sequence of 32 chips is cyclically shifted to generate the entire 32-symbol alphabet.

The system uses a Reed-Solomon code for channel encoding. (The reader is referred to Macwilliams & Sloane [1] for a discussion on the Reed-Solomon codes.) An R-S (31,15) code is used to encode 15 information symbols into 31 channel symbols, so that 16 symbols are used for error correction and error detection purposes. The code allows for forward-error correction if

$$2e + E < 17 \qquad (1\text{-}1)$$

where e = the number of symbol errors and E = the number of symbol erasures within the 31-symbol code word. If

$$2e + E \geq 17 \qquad (1\text{-}2)$$

then a decoding error will occur.

The probability of a word error (P_w), or the expected relative frequency of a word decoding error, where a word is represented by an R-S (31,15) code, can be formulated using the probability of a symbol error (P_e) and the probability of a symbol erasure (P_E) as independent variables. But P_E and P_e are not independent variables: they are dependent upon the signal-to-noise ratio (SNR), the modulation technique used, and the threshold setting for the decision rule used. Nevertheless, constant P_w curves as a function of P_E and P_e can be plotted on log x log graph paper. The set of P_w curves becomes a powerful tool when used in conjuction with the P_E vs. P_e plot with constant SNR

curves, because by superimposing the curves we can relate SNR to P_w.

Decision rules for detection of spread spectrum signals were investigated. Decision rules were designed using simple and ratio thresholding techniques. For each decision rule, the performance of the detection system in terms of P_E and P_e was analyzed. The obtained data were used to plot constant SNR curves and constant threshold curves. With the use of the P_w curves the optimum threshold setting was found for a given SNR.

Orthogonal signalling (FSK) and antipodal signalling (PSK) were investigated to determine their effects on the performance of the detection system.

Analog and digital correlations were considered. The performance curves of analog correlation and digital correlation were compared.

Monte Carlo simulation of the digital detection process using the threshold decision rule was used to produce the performance data which can be compared with the results of the analysis.

CHAPTER 2

DETECTION THEORY APPLIED TO 32-ARY ORTHOGONAL SIGNALS

For radio communications, a transmitted signal becomes corrupted with an additive gaussian white noise when it reaches its destination. Because a signal attenuates during its propagation, signal degradation due to the presence of the noise in the signal becomes a problem especially for long distance transmissions. Because the white gaussian noise is a random process, the likelihood of a detection error occurring is described in terms of the probability of an (detection) error.

A received signal is represented by

$$y(t) = x(t) + n_w(t) \tag{2-1}$$

where $x(t)$ is the transmitted signal and $n_w(t)$ is the gaussian white noise. The noise $n_w(t)$ is assumed to have the white spectral density

$$G(f) = N_o/2. \tag{2-2}$$

The receiver operates on the received signal $y(t)$ to determine which of the symbols μ_i, $i=1,2,\ldots,M$, were sent.

If μ_i is a symbol belonging to the set

$$U = \{\mu_1, \mu_2, \ldots, \mu_M\}, \tag{2-3}$$

then μ_i is an M-ary symbol that is equivalent to $\log_2(M)$ bits of information.

The spread spectrum communication system in our study uses 32-ary symbols, each symbol representing 5 bits of information; 32 chips are used to generate a signal $x_i(t)$ representing μ_i (for i=1,2,...,32).

Thirty-two chips are capable of generating 2^{32} different signals; however, among the 2^{32} prospective signals, only 32 which are orthogonal to each other are chosen. There are various ways of generating 32-ary orthogonal signals, and we will explore two of the methods in Chapter 6.

Suppose there exists a set of 32 orthogonal signals described by

$$X = \{x_1(t), x_2(t), \ldots, x_{32}(t)\}. \qquad (2\text{-}4)$$

A set of vectors

$$V = \{\phi_1(t), \phi_2(t), \ldots, \phi_{32}(t)\} \qquad (2\text{-}5)$$

forms the basis of the vector space ζ_{32} of dimension 32 which is spanned by the linearly independent vectors $x_1(t), x_2(t), \ldots, x_{32}(t)$. Each signal $x_i(t)$ is a linear combination of $\phi_1, \phi_2, \ldots, \phi_{32}$ such that

$$x_i(t) = x_{i1}\phi_1 + x_{i2}\phi_2 + \ldots + x_{i32}\phi_{32} \qquad (2\text{-}6)$$

where $x_{i1}, x_{i2}, \ldots, x_{i32}$ are scalars. The orthogonality of the signals implies that

$$\langle x_i, x_i \rangle = E_s \qquad i=1,2,\ldots,32 \qquad (2\text{-}7a)$$

$$\langle x_i, x_j \rangle = 0 \qquad i \neq j. \qquad (2\text{-}7b)$$

2.1 Signal Space Formulation

The present discussion of signal space formulation is limited to the case of having 32-ary orthogonal signals. The reader is referred to Carlson [2] for a generalized treatment of signal space formulation.

Suppose there are 32 orthogonal signals $x_1(t)$, $x_2(t)$, ..., $x_{32}(t)$. Then there exists a signal space ζ_{32} containing all of the above signals; ζ_{32} is spanned by an orthonormal basis $\{\phi_1(t), \phi_2(t), \ldots, \phi_{32}(t)\}$, so that

$$x_i(t) = \sum_{k=1}^{32} x_{ik}\phi_k(t) \qquad (2\text{-}8)$$

where

$$x_{ik} = \langle x_i, \phi_k \rangle = \int_{-\infty}^{\infty} x_i(t)\ \phi_k(t)dt. \qquad (2\text{-}9)$$

An additive zero-mean gaussian white noise present in the transmission medium may not be fully contained in ζ_{32}, in which case it cannot be fully described by a linear combination of the orthonormal basis vectors $\phi_1(t)$, $\phi_2(t)$, ..., $\phi_{32}(t)$ spanning the signal space ζ_{32}. But the noise $n_w(t)$ can be described as a sum of two terms, one term representing the component vector which does belong to ζ_{32} and the other term representing the component vector which does not belong to ζ_{32}. The noise can be represented as

$$n_w(t) = n(t) + n_e(t) \qquad (2\text{-}10)$$

where $n(t)$ is the projection of the vector $n_w(t)$ on ζ_{32} and $n_e(t)$ is the

irrelevant noise.

The relevant noise n(t) is a linear combination of the basis vectors and is described by

$$n(t) = \sum_{k=1}^{32} n_k \phi_k(t) \qquad (2\text{-}11)$$

where

$$n_k(t) = \langle n, \phi_k \rangle = \langle n_w, \phi_k \rangle. \qquad (2\text{-}12)$$

Whereas, for the irrelevant noise,

$$\langle n_e, \phi_k \rangle = 0 \qquad k=1,2,\ldots 32 \qquad (2\text{-}13)$$

because $n_e(t)$ does not belong to the signal space ζ_{32}.

The detector for the system in our study has a bank of 32 correlators. A received signal is correlated with 32 seperate locally generated signals so that

$$\begin{aligned} \langle y, x_1 \rangle &= r_1 \\ \langle y, x_2 \rangle &= r_2 \\ &\vdots \\ \langle y, x_{32} \rangle &= r_{32} \end{aligned} \qquad (2\text{-}14)$$

where r_k is the output of the k'th correlator.

Note that

$$y(t) = x_i(t) + n_w(t) = x_i(t) + n(t) + n_e(t) \qquad (2\text{-}15)$$

Therefore, substituting for y(t),

$$\langle y, x_j \rangle = \langle x_i + n + n_e, x_j \rangle \tag{2-16a}$$

$$\langle y, x_j \rangle = \langle x_i, x_j \rangle + \langle n, x_j \rangle + \langle n_e, x_j \rangle. \tag{2-16b}$$

But

$$\langle n_e, x_j \rangle = \emptyset \tag{2-17}$$

so

$$\langle y, x_j \rangle = \langle x_i, x_j \rangle + \langle n, x_j \rangle \tag{2-18a}$$

$$\langle y, x_j \rangle = \langle x_i + n, x_j \rangle. \tag{2-18b}$$

Defining z(t) as the projection vector of y(t) on ζ_{32},

$$z(t) = x_i(t) + n(t) \tag{2-19}$$

and

$$\langle y, x_j \rangle = \langle z, x_j \rangle. \tag{2-20}$$

Assuming that only hard decisions are made, the symbol μ_j corresponding to the signal $x_j(t)$ to which z(t) lies closest in the signal space ζ_{32} is chosen. For z(t) to lie closest to $x_j(t)$ the following condition must be satisfied:

$$\|z - x_j\| < \|z - x_i\| \qquad \text{all } i \neq j. \tag{2-21}$$

If $x_j(t)$ is the transmitted signal, then

$$z(t) - x_j(t) = n(t) \tag{2-22}$$

and

$$\|z-x_j\| = \|n\|. \tag{2-23}$$

where

$$\|n\| = \langle n,n\rangle^{1/2}. \tag{2-24}$$

The inner product of the relevant noise with itself is the sum of the magnitude squared of the component vectors as follows:

$$\langle n,n\rangle = \langle n_1\phi_1+n_2\phi_2+ \ldots +n_{32}\phi_{32}, n_1\phi_1+n_2\phi_2+ \ldots +n_{32}\phi_{32}\rangle \tag{2-25a}$$

$$\langle n,n\rangle = n_1^2 + n_2^2 + \ldots + n_{32}^2 \tag{2-25b}$$

where each n_i has the following statistical variance:

$$\sigma^2_{n_i} = E[n_i - E[n_i]]^2 \tag{2-26a}$$

$$\sigma^2_{n_i} = \overline{n_i^2} - \overline{n_i}^2. \tag{2-26b}$$

But

$$\overline{n_i} = \overline{\langle n_w,\phi_i\rangle} \tag{2-27}$$

and

$$\overline{n_w} = 0 \tag{2-28}$$

because $n_w(t)$ is a zero-mean gaussian white noise. Therefore,

$$\overline{n_i} = 0. \tag{2-29}$$

Using (2-29), (2-26b) is simplified as

$$\sigma_{n_i}^2 = \overline{n_i^2}. \tag{2-30}$$

The term $\overline{n_i^2}$, which can be written as $E[n_i^2]$, is analyzed by first deriving the relationship for $E[n_i n_j]$. $E[n_i n_j]$ is defined as

$$E[n_i n_j] = E\left[\int_{-\infty}^{\infty} n_w(t)\phi_i(t)dt \int_{-\infty}^{\infty} n_w(l)\phi_m(l)dl\right]. \tag{2-31}$$

But since only $n_w(t)$ and $n_w(l)$ are random variables $E[n_i n_j]$ can be rewritten as

$$E[n_i n_j] = \int_{-\infty}^{\infty}\int_{-\infty}^{\infty} E[n_w(t)n_w(l)]\phi_i(t)\phi_j(l)dtdl. \tag{2-32}$$

$E[n_w(t)n_w(l)]$ can be represented as an inner product of $n_w(t)$ and $n_w(l)$ as

$$E[n_w(t)n_w(l)] = \langle n_w(t), n_w(l)\rangle \tag{2-33}$$

$$E[n_w(t)n_w(l)] = \langle n_w(t), n_w(t-(t-l))\rangle. \tag{2-34}$$

Noting that

$$R_{n_w}(t-l) = \langle n_w(t), n_w(t(t-l))\rangle \tag{2-35}$$

a new relationship for $E[n_w(t)n_w(l)]$ is found as follows:

$$E[n_w(t)n_w(l)] = R_{n_w}(t-l). \tag{2-36}$$

The autocorrelation of white noise is

$$R_{n_w}(\tau) = (N_o/2)\delta(\tau). \tag{2-37}$$

Substituting $(N_o/2)\delta(t-1)$ for $R_{n_w}(t-1)$ in (2-36),

$$E[n_w(t)n_w(1)] = (N_o/2)\ \delta(t-1) \tag{2-38}$$

Furthermore, substituting $(N_o/2)\delta(t-1)$ for $E[n_w(t)n_w(1)]$ in (2-32),

$$E[n_i n_j] = (N_o/2)\int_{-\infty}^{\infty}\int_{-\infty}^{\infty}\phi_i(t)\phi_j(1)\delta(t-1)dtd1. \tag{2-39}$$

Since $\phi_i(t)$ and $\phi_j(1)$ are orthonormal vectors, (2-39) can be simplified as

$$E[n_i n_j] = \begin{cases} N_o/2 & i=j \\ \emptyset & i\neq j. \end{cases} \tag{2-40}$$

We note that for the case of i=j

$$E[n_i^2] = \overline{n_i^2} = N_o/2. \tag{2-41}$$

By substituting $N_o/2$ for $\overline{n_i^2}$ in (2-3$\emptyset$) we get

$$\sigma_{n_i}^2 = N_o/2. \tag{2-42}$$

Note that n_i is a statistically independent gausssian variate with variance $N_o/2$. The probability density function of n_i is

$$P_{n_i}(n_i) = (\pi N_o)^{-1/2}\exp[-n_i^2/N_o] \tag{2-43}$$

which is used to substitute for P_{n_1}, P_{n_2}, ..., $P_{n_{32}}$ in

$$P_n(n) = P_{n_1}(n_1)P_{n_2}(n_2)\ldots P_{n_{32}}(n_{32}) \tag{2-44}$$

to get

$$P_n(n) = (\pi N_o)^{-16}\exp[-\|n\|^2/N_o] \tag{2-45}$$

where

$$\|n\|^2 = n_1^2 + n_2^2 + \ldots + n_{32}^2. \tag{2-46}$$

2.2 Maximum Likelihood Decision Rule

Given a projection vector z(t), it is possible to choose the signal most likely to have been transmitted. We impose the condition

$$P(\mu_j|z) > P(\mu_i|z) \qquad \text{all } i \neq j \qquad (2\text{-}47)$$

which, if satisfied, allows us to decide that μ_j is the most likely symbol to have been transmitted.

Using the Bayes' rule

$$P(\mu_i|z) = P(\mu_i)P_z(z|\mu_i)/P_z(z) \qquad (2\text{-}48)$$

(2-47) is restated as

$$P(\mu_j)P_z(z|\mu_j) > P(\mu_i)P_z(z|\mu_i) \qquad \text{all } i \neq j. \qquad (2\text{-}49)$$

Assuming that every symbol has an equal probability of being transmitted, (2-49) is simplified as

$$P_z(z|\mu_j) > P_z(z|\mu_i) \qquad \text{all } i \neq j. \qquad (2\text{-}50)$$

Since z(t) given μ_i implies

$$n(t) = z(t) - x_i(t) \qquad (2\text{-}51)$$

where μ_i is represented by $x_i(t)$, $P_z(z|\mu_i)$ can be written as

$$P_z(z|\mu_i) = P_n(z-x_i). \qquad (2\text{-}52)$$

Using (2-45) and (2-52) we get

$$P_z(z|\mu_i) = (\pi N_o)^{-16}\exp[-\|z-x_i\|^2/N_o] \tag{2-53}$$

and using (2-50) and (2-53) we get

$$\exp[-\|z-x_j\|^2/N_o] > \exp[-\|z-x_i\|^2/N_o] \tag{2-54}$$

which is simplified as

$$\|z-x_j\|^2 < \|z-x_i\|^2 \qquad \text{all } i\neq j \tag{2-55}$$

where

$$\|z-x_i\|^2 = \langle z-x_i, z-x_i\rangle \tag{2-56}$$

$$\langle z-x_i, z-x_i\rangle = \|z\|^2 - 2\langle z, x_i\rangle - \|x_i\|^2. \tag{2-57}$$

The energies for the signals $z(t)$ and $x_i(t)$ are defined as

$$E_z = R_z(0) = \|z\|^2 \tag{2-58a}$$

$$E_{x_i} = R_{x_i}(0) = \|x_i\|^2. \tag{2-58b}$$

Using the above definitions, (2-57) is restated as

$$\langle z-x_i, z-x_i\rangle = E_z - 2\langle z, x_i\rangle + E_{x_i} \tag{2-59}$$

which is equivalent to

$$\langle z-x_i, z-x_i\rangle = E_z - 2\langle y, x_i\rangle + E_{x_i} \tag{2-60}$$

because

$$\langle z, x_i\rangle = \langle y-n_e, x_i\rangle = \langle y, x_i\rangle. \tag{2-61}$$

Equations (2-55), (2-56), and (2-60) are used to get

$$\langle z,x_j\rangle - (1/2)E_j \;>\; \langle z,x_i\rangle - (1/2)E_i \qquad \text{all } i\neq j. \tag{2-62}$$

But we have a signal set whose 32 orthogonal signals have the property

$$E_1 = E_2 = \ldots = E_{32}. \tag{2-63}$$

When (2-63) is considered, (2-62) simplifies to

$$\langle z,x_j\rangle \;>\; \langle z,x_i\rangle \qquad \text{all } i\neq j. \tag{2-64}$$

To choose the symbol most likely to have been sent, the modified decision function is defined as

$$D_i' = \langle z,x_i\rangle = \langle y,x_i\rangle \tag{2-65}$$

and μ_j is chosen such that

$$D_j' > D_i' \qquad \text{all } i\neq j. \tag{2-66}$$

2.3 Decision Rules Utilizing the Erasure Symbols

The detector in our study is capable of declaring symbol erasures. A symbol erasure is declared when the received signal y(t) has unacceptably degraded in signal quality due to the noise present in the transmission medium. Expressed in another way, a symbol erasure is declared when the probability of a symbol error becomes unacceptably high.

For the case of having a detector which is capable of declaring erasures, the function of the decision rule is not to minimize the P_e, but to find the optimum ratio of P_E to P_e. Unfortunately, the optimum ratio is not fixed, it is dependent upon SNR, the modulation technique used, and the decision rule used.

The materials subsequent to Chapter 3 will analyze the optimization of detection performance using different options in the decision rule used, modulation technique used, and the correlation method used. But we will first investigate P_w as a function of P_E and P_e.

CHAPTER 3

PROBABILITY OF A WORD ERROR

The discussion in this chapter is based on a report by Rosenstark and Frank [3].

In this chapter, the term word error refers to the decoding error of a Reed-Solomon (31,15) code. Thirty-one detected symbols, each of which may be a correct symbol, a wrong symbol, or an erasure, are processed by the decoder to generate a word consisting of 15 information symbols. The decoded word, however, can be in error when there exists enough symbol errors and erasures. This chapter studies the relationships among P_E, P_e, and P_w.

The system in our investigation uses the Reed-Solomon (R-S) coding. The R-S (31,15) decoder is capable of error-free decoding if

$$2e + E < 17 \tag{3-1}$$

where

$$e = \text{the number of symbol errors,} \tag{3-2a}$$

$$E = \text{the number of symbol erasures.} \tag{3-2b}$$

A word (code) error occurs if

$$2e + E = S \tag{3-3a}$$

where

$$S \geq 17. \tag{3-3b}$$

Table 3.1. Some Combinations of Errors and Erasures Which Cause Code Word Errors

2e+E=17		2e+E=18		2e+E=19		2e+E=20	
e	E	e	E	e	E	e	E
0	17	0	18	0	19	0	20
1	15	1	16	1	17	1	18
2	13	2	14	2	15	2	16
3	11	3	12	3	13	3	14
4	9	4	10	4	11	4	12
5	7	5	8	5	9	5	10
6	5	6	6	6	7	6	8
7	3	7	4	7	5	7	6
8	1	8	2	8	3	8	4
		9	0	9	1	9	2
						10	0

Defining e_{min} as the minimum number of symbol errors required for a word error to occur, we see from table 3.1 that

$$e_{min} = 0 \tag{3-4}$$

for at least S equal to 17, 18, 19, and 20. We will define e_{max} as the maximum number of symbol errors for a given value of S. An inspection of table 3.1 shows that

$$e_{max} \leq S/2. \tag{3-5a}$$

It is also apparent that

$$e_{max} = \lfloor S/2 \rfloor \tag{3-5b}$$

where $\lfloor x \rfloor$, the floor of x, is defined as the largest integer less than or equal to x (the definition appears in Iverson [4]).

When a signal is detected, a symbol decision is made. The decision can be correct, be in error, or be declared an erasure. The sum of the number of errors and the number of erasures in an R-S (31,15) word cannot exceed the total number of symbols in the word (there are 31 symbols in an R-S (31,15) code word), or

$$e + E \leq 31 \tag{3-6}$$

which can be restated as

$$E \leq 31 - e. \tag{3-7}$$

Using (3-3a), the above becomes

$$E = S - 2e. \tag{3-8}$$

Using (3-7) and (3-8) we arrive at the relationship

$$e \geq S - 31. \tag{3-9}$$

In the above, e must be a non-negative integer, therefore, e_{min} is defined for two different cases as follows:

$$e_{min} = \begin{cases} S - 31 & \text{if } S > 31 \\ \emptyset & \text{if } S \leq 31. \end{cases} \tag{3-10}$$

Referring to (3-6), the maximum possible value of e is 31. By substituting 31 for e_{max} in (3-5b) we get

$$\max\{S\} = 2(31) = 62. \tag{3-11}$$

For a word error to occur, S must be an integer that takes on the following relationship:

$$17 \leq S \leq 62. \tag{3-12}$$

The probability of a word error is defined as

$$P_w = \sum_{S=17}^{62} P(S) \tag{3-13}$$

where P(S) is

$$P(S) = \sum_{k=e_{min}}^{e_{max}} P(S \cap e=k). \tag{3-14}$$

Since e_{min} in (3-10) exists for two different cases, P(S) also exists for two different cases as follows:

$$P(S) = \begin{cases} \sum_{k=S-31}^{S/2} P(S \cap e=k) & \text{if } S \geq 31 \\ \sum_{k=\emptyset}^{S/2} P(S \cap e=k) & \text{if } S \leq 31 \end{cases} \tag{3-15}$$

where substitutions are made for e_{max} and e_{min} using (3-5b) and (3-10). $P(S \cap e=k)$ is defined as

$$P(S \cap e=k) = \binom{31}{K} P_e^k \binom{31-k}{S-2K} P_E^{S-2k} \binom{31-S+k}{31-S+K} P_C^{31-S+k} \tag{3-16}$$

where

$$P_e = \text{probability of a symbol error,} \tag{3-17a}$$

$$P_E = \text{probability of a symbol erasure,} \tag{3-17b}$$

$$P_C = \text{probability of a correct symbol.} \tag{3-17c}$$

Noting that

$$\binom{31-S+k}{31-S+k} = 1, \tag{3-18}$$

(3-16) is simplified as

$$P(S \cap e=k) = \binom{31}{k} \binom{31-k}{s-2k} P_e^k P_E^{S-2k} P_C^{31-S+k}. \tag{3-19}$$

But

$$\binom{31}{k} \binom{31-k}{S-2k} = \frac{31!}{(31-k)!k!} \frac{(31-k)!}{(31-S+k)!(S-2k)!} \tag{3-20a}$$

$$\binom{31}{k} \binom{31-k}{S-2k} = \frac{31!}{k!(S-2k)!(31-S+k)}. \tag{3-20b}$$

and

$$P_C = 1 - (P_e+P_E). \tag{3-21}$$

Using (3-19), (3-20b), and (3-21) we get

$$P(S \cap e=k) = \frac{31! P_e^k P_E^{S-2k} [1-(P_e+P_E)]^{31-S+k}}{k!(S-2k)!(31-S+k)!}. \tag{3-22}$$

Using (3-13) and (3-15) we write P_w as

$$P_w = \sum_{S=17}^{31} \sum_{k=0}^{S/2} P(S \cap e=k) + \sum_{S=32}^{62} \sum_{k=S-31}^{S/2} P(S \cap e=k) \qquad (3\text{-}23)$$

where $P(S \cap e=k)$ is defined by (3-22).

P_w as a function of P_E and P_e can be numerically analyzed using (3-22) and (3-23). The obtained data can be plotted in the form P_E vs. P_e for constant P_w. This was done for the values

$$P_w = 10^{-2}, 10^{-3}, \ldots, 10^{-10} \qquad (3\text{-}24)$$

in fig. 3.1. The P_w curves can be used as a tool to compare the performances of various decision rules under various detector operating conditions.

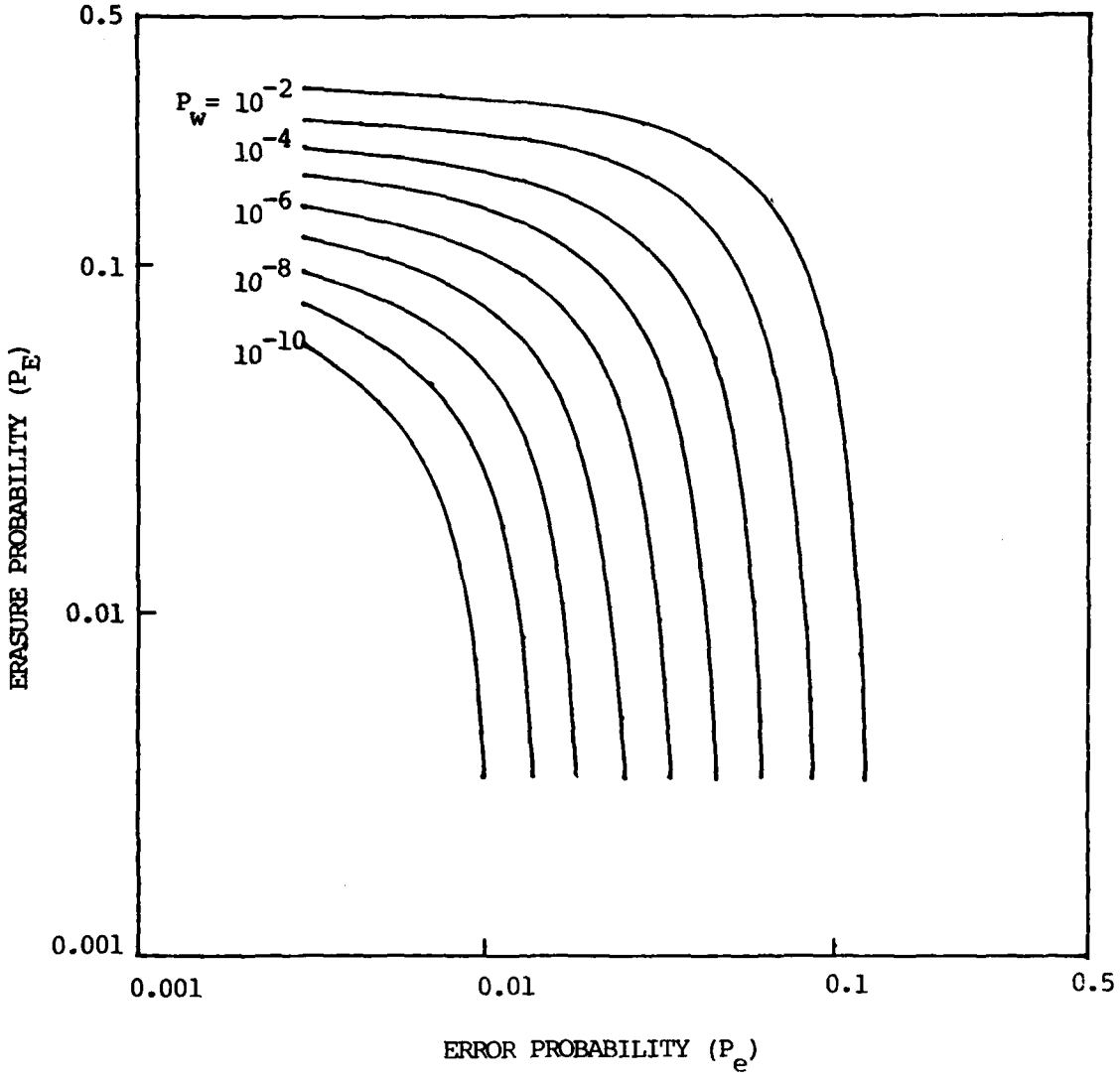

Figure 3.1. Probability-of-a-word-error curves.

CHAPTER 4

ANALOG SIGNAL DETECTION

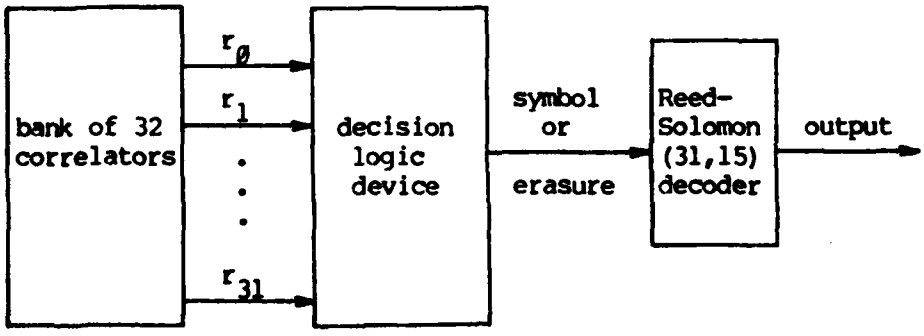

Figure 4.1. Diagram of detector and decoder.

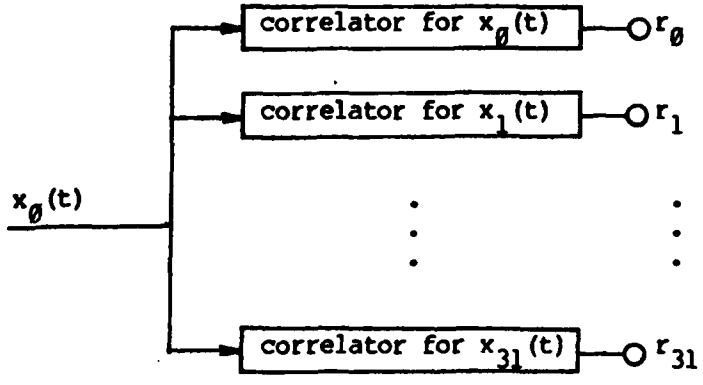

Figure 4.2. 32 correlator detection system.

Figure 4.1 illustrates the detection and decoding processes considered in this chapter. The noise corrupted signal y(t) is processed by the bank of 32 correlators illustrated in fig. 4.2. Each correlator produces a correlator output r_j which is sent to the decision logic device. The device takes the 32 correlator outputs and decides upon a symbol belonging to the set

$$U = \{\mu_0, \mu_1, \ldots, \mu_{31}, \text{erasure}\}. \qquad (4\text{-}1)$$

The decoder receives the symbols until the 31 symbols making up a code word are received. Forward-error correction is performed on the R-S (31,15) code word, and the 15 information symbols are outputted.

Two different decision rules were developed and analyzed. The decision rules studied are the threshold rule and the ratio rule.

4.1 Threshold Rule

One variation of the threshold rule works as follows: If only one correlator output equals or exceeds the threshold, then declare the symbol corresponding to the largest correlator output as the received symbol. If the above condition is not met, then declare an erasure.

This decision rule has a major flaw because the condition that only one correlator output must equal or exceed the threshold for a symbol decision to occur causes the likelihood of an erasure occurring to substantially exceed the likelihood of a symbol error occurring for the SNR ranges of our interest. After reviewing the results of an initial numerical analysis, the analysis of this decision rule was discontinued.

The second version of the threshold rule, which later proved to yield a proper balance of symbol erasures and symbol errors, works as follows: If one or more correlator outputs equal or exceed the threshold, then declare the

symbol corresponding to the largest correlator output as the received symbol. If either the largest correlator output does not exceed the threshold, or if we have a draw, then declare an erasure.

Note that the threshold setting is variable. Its variability serves to control the ratio of P_E to P_e. If the incoming signal is weak, or if the SNR is low, then the threshold should be set relatively low to prevent an excessive occurrence of symbol erasures. But if the incoming signal is strong, or the SNR is high, then the threshold should be set relatively high so that the maximum correlation values which are relatively low can be declared as erasures. Under the condition of a changing SNR, the threshold setting must also change to achieve an optimum word error performance. We will later see that this is not the case for the ratio rule. The distinct advantage of the ratio rule over the threshold rule is that its optimum ratio setting stays relatively fixed for the range of SNR of our interest.

The performance for the detection system using the threshold rule for its decision logic device is analyzed for orthogonal signalling and antipodal signalling. For an informative discussion on the signalling techniques the reader is referred to Pasupathy [5].

4.1.1 Analysis of the Threshold Rule Performance for Orthogonal Signalling

Without going in depth into the correlation analysis we will state that when an FSK modulated chip signal is correlated with a reference FSK modulated chip signal, we get

$$r_c = \begin{cases} E_c & \text{if the chips have the same frequency} \\ \emptyset & \text{if the chips have different frequencies} \end{cases} \qquad (4\text{-}2)$$

where r_c is the chip correlator output variable and E_c is the energy of the FSK modulated chip signal.

Suppose a noiseless signal $x_i(t)$ is received. Because the signal consists of 32 modulated chips, the i'th correlator peak output will be

$$r_i = 32E_c = E_s \qquad (4\text{-}3a)$$

where r_i is the correlator output and E_s is the energy of the signal $x_i(t)$. But if $x_i(t)$ is correlated by a j'th correlator (where $i \neq j$), then the correlator output will be

$$r_j = 16E_c = (1/2)E_s . \qquad (4\text{-}3b)$$

A code word c_i consisting of 32 (bipolar) chips becomes a signal $x_i(t)$ when modulated. When c_i is correlated with c_j (where $i \neq j$), 16 chip positions will have the chips of same polarity and the remaining 16 chip positions will have the chips of opposite polarity (the reader can verify this by using the modified maximal-length sequences in figure 6.3 or the Welti codes in figure 6.5). When c_i is correlated with itself, all 32 chip positions will have the

chips of same polarity. Using (4-2) it can be seen that (4-3a) and (4-3b) are true.

Given that every signal $x_i(t)$ (for $i=0,1,\ldots,31$) has an equal probability of being transmitted, we will assume throughout this report that $x_0(t)$ is transmitted without any loss of generality.

Zero-mean white gaussian noise present in the transmission medium is also assumed throughout the paper. For orthogonal signalling, r_0 is gaussianly distributed around the mean energy value of E_s with variance $E_sN_o/2$. The other correlator outputs are similarly gaussianly distributed, but the distributions have the mean value of $(1/2)E_s$.

To get an erasure we must have

$$r_o < tE_s \qquad (4\text{-}4a)$$

$$r_i < tE_s \qquad \text{all } i\neq 0 \qquad (4\text{-}4b)$$

where t is the threshold variable and

$$0 < t \leq 1. \qquad (4\text{-}5)$$

The probability of an erasure is formulated as

$$P_E = Q[(1-t)E_s/\sigma]\{1-Q[(t-1/2)E_s/\sigma]\}^{31} \qquad (4\text{-}6)$$

where Q[x] is the probability that a gaussianly distributed variable X exceeds the value x (refer to Abramowitz & Stegun [6]).

A correct decision takes place when

$$r_{\emptyset} = y \tag{4-7a}$$

$$r_i < y \qquad i=1,2,\ldots,31 \tag{4-7b}$$

and

$$y \geq tE_s. \tag{4-8}$$

The probability of a correct decision is formulated as

$$P_c = \frac{1}{\sqrt{2\pi}\,\sigma} \int_{tEs}^{\infty} e^{-(y-Es)^2/2\sigma^2} \{1-Q[(y-E_s/2)/\sigma]\}^{31} dy. \tag{4-9}$$

Three types of a decision can be made by a decision logic device: a right decision, a wrong decision, and a decision to declare an erasure. Regardless of the probability of each event, the probability of any of the three events occurring is 1, or

$$1 = P_e + P_E + P_c. \tag{4-10a}$$

When P_E and P_c are known, the probability of an error is determined by using the relationship in (4-10a) as follows:

$$P_e = 1 - P_E - P_c. \tag{4-10b}$$

Substituting for P_E and P_c in (4-10b) using (4-6) and (4-9) we get

$$P_e = 1-Q[(1-t)E_s/\sigma]\{1-Q[(t-1/2)E_s/\sigma]\}^{31}$$

$$-\frac{1}{\sqrt{2\pi}\,\sigma} \int_{tE_s}^{\infty} e^{-(y-E_s)^2/2\sigma^2} \{1-Q[(y-F_s/2)/\sigma]^{31}\} dy. \tag{4-11}$$

The terms in (4-11) can be rearranged to yield

$$P_e = Q[(1-t)E_s/\sigma][1-\{1-Q[(t-1/2)E_s/\sigma]\}^{31}]$$

$$-\frac{1}{\sqrt{2\pi}\,\sigma}\int_{tE_s}^{\infty} e^{-(y-E_s)^2/2\sigma^2}[1-\{1-Q[(y-E_s/2)/\sigma]\}^{31}]dy. \quad (4\text{-}12)$$

For very small values of Q which correspond to small values of P_e we can use the two-term binomial expansion

$$(1+x)^k \simeq 1 + kx \quad (4\text{-}13)$$

in (4-12) to obtain

$$P_e = 31Q[(1-t)E_s/\sigma]Q[(t-1/2)E_s/\sigma]$$

$$+\frac{31}{\sqrt{2\pi}\,\sigma}\int_{tE_s}^{\infty} e^{-(y-E_s)^2/2\sigma^2}Q[(y-E_s/2)/\sigma]dy. \quad (4\text{-}14)$$

Noting that

$$\sigma = \sqrt{E_s N_o/2} \quad (4\text{-}15)$$

and

$$E_s/\sigma = \sqrt{2E_s/N_o} \quad (4\text{-}16)$$

(4-6), (4-12), and (4-14) are numerically computed. With the obtained data, P_E vs. P_e for constant values of E_s/N_o (SNR) were plotted in figure 4.3. The loci of the constant t are also shown. Superimposing the P_w curves from figure 3.1 on the above curves enables us to predict the detection system performance.

An examination of figure 4.3 reveals that we should set the threshold at approximately t=Ø.8 to minimize the word error probability. Furthermore, we observe that the change in word error probability is minimal as long as Ø.7 < t < Ø.82, so the threshold can change an appreciable amount before large changes take place in system performance.

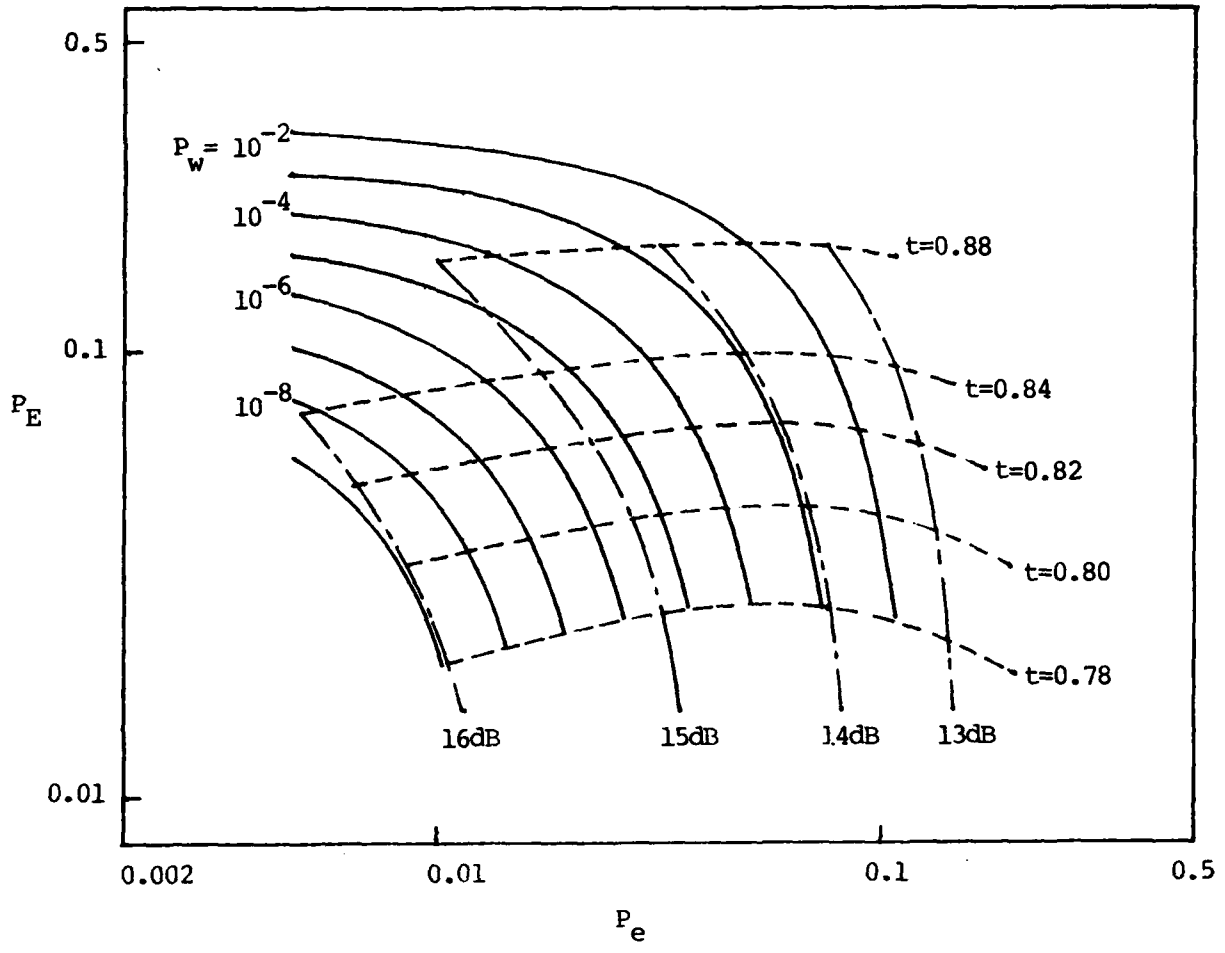

Figure 4.3. Threshold rule orthogonal signalling performance curves.

4.1.2 Analysis of the Threshold Rule Performance for Antipodal Signalling

Without going in depth into the correlation analysis we will state that when a PSK modulated chip signal is correlated with a reference PSK modulated chip signal, we get

$$r_c = \begin{cases} E_c & \text{if the chips have the same polarity} \\ -E_c & \text{if the chips have the opposite polarity} \end{cases} \qquad (4\text{-}17)$$

where r_c is the chip correlator output variable and E_c is the energy of the PSK modulated chip signal.

Suppose a noiseless signal $x_i(t)$ is received. Because the signal consists of 32 modulated chips, the i'th correlator peak output will be

$$r_i = 32E_c = E_s \qquad (4\text{-}18a)$$

where r_i is the symbol correlator output variable and E_s is the energy of the signal $x_i(t)$. But if the j'th correlator correlates the signal $x_i(t)$ (where $i \neq j$), the correlator output will be

$$r_j = 0. \qquad (4\text{-}18b)$$

A code word c_i consisting of 32 (bipolar) chips becomes a signal $x_i(t)$ when modulated. When c_i is correlated with c_j (where $i \neq j$), 16 chip positions will have chips of same polarity and the remaining 16 chip positions will have chips of opposite polarity (the reader can verify this by using the modified maximal-length sequences in figure 6.3 or the Welti codes in figure 6.5).

When c_i is correlated with itself, all 32 chip positions will have chips of same polarity. Using (4-17), it can be seen that (4-18a) and (4-18b) are true.

The probability analysis for antipodal signalling is essentially the same as the analysis for orthogonal signalling, but the statistical mean value for r_i (for i=1,2,...,31) is zero for antipodal signalling. Without retracing the derivations we will simply state the necessary relationships as follows:

$$P_E = Q[(1-t)E_s/\sigma]\{1-Q[tE_s/\sigma]\}^{31} \qquad (4\text{-}19)$$

$$P_c = \frac{1}{\sqrt{2\pi}\,\sigma}\int_{tE_s}^{\infty} e^{-(y-E_s)^2/2\sigma^2}\{1-Q[y/\sigma]\}^{31}dy \qquad (4\text{-}20)$$

$$P_e = Q[(1-t)E_s/\sigma][1-\{1-Q[tE_s/\sigma]\}^{31}]$$
$$-\frac{1}{\sqrt{2\pi}\,\sigma}\int_{tE_s}^{\infty} e^{-(y-E_s)^2/2\sigma^2}[1-\{1-Q[y/\sigma]\}^{31}]dy. \qquad (4\text{-}21)$$

Using the definition in (4-16), (4-19) and (4-21) can be numerically computed. By plotting the curves as was done for orthogonal signalling we are able to predict the probability of a word error.

The curves derived from the numerical analysis are shown in fig. 4.4. We see that a threshold setting of t=0.58 yields low word error probabilities. If t is varied over the range $0.5 < t < 0.62$ the effect on word error probability will be minimal.

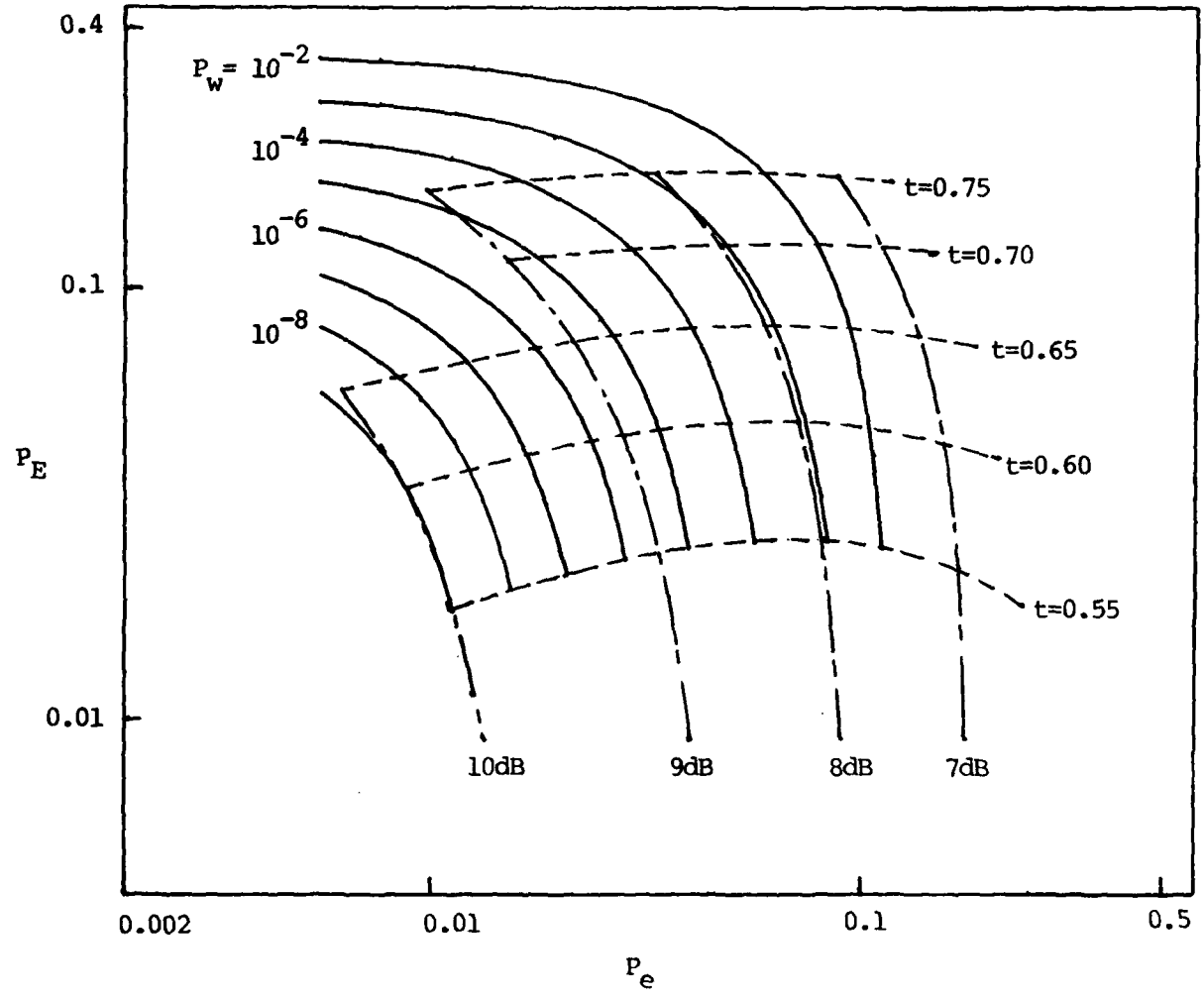

Figure 4.4. Threshold rule antipodal signalling performance curves.

4.2 Ratio Rule

The threshold rule was a good decision rule to implement because the variable threshold setting allowed for the control over the ratio of the probability of an erasure to the probability of an error. But we noted that the optimum threshold setting varies with the SNR of the received signal.

We pursued our investigation to find a decision rule whose optimum threshold setting stays fixed when the SNR of the received signal varies. The decision rule that satisfies the requirement is the ratio rule. The ratio rule works as follows: Take the ratio of the largest correlator output to the next largest output. If the ratio does not equal or exceed the ratio setting d, which is a variable which takes on a value greater than 1.0, then declare an erasure. If the ratio is equal to or greater than d, then declare the symbol corresponding to the largest correlator output as the transmitted symbol.

The ratio rule word error performance for analog correlation is analyzed for orthogonal signalling and antipodal signalling.

4.2.1 Analysis of the Ratio Rule Performance for Orthogonal Signalling

For the present analysis of the ratio rule performance, (4-2) and (4-3) hold true.

To get a correct symbol decision, $r_\emptyset$ must be the largest correlator output, and it must exceed the next largest correlator output by a factor d; $r_\emptyset$ is gaussianly distributed around the mean energy value of E_s with variance $E_sN_o/2$. The other correlator outputs are similarly gaussianly distributed, but the distributions have the mean value of $(1/2)E_s/N_o$. The probability of a correct decision is

$$P_c = \frac{1}{\sqrt{2\pi}\,\sigma}\int_{-\infty}^{\infty} e^{-(r-E_s)^2/2\sigma^2}\{1-Q[(r/d-E_s/2)/\sigma]\}^{31}dr. \qquad (4\text{-}22)$$

An error occurs if any of the 31 correlators, other than the $\emptyset$'th correlator, gives rise to an output r_i, i=1,2,...,31, which exceeds the second largest correlator output by a factor d. The probability of this occurring is

$$P_e = \frac{31}{\sqrt{2\pi}\,\sigma}\int_{-\infty}^{\infty} e^{-(r-E_s/2)^2/2\sigma^2}\{1-Q[(r/d-E_s/2)/\sigma]\}^{30}\{1-Q[(r/d-E_s)/\sigma]\}dr. \qquad (4\text{-}23)$$

To find the probability of an erasure we take the probability of a correct decision and the probability of an error and express the probability of an erasure as follows:

$$P_E = 1 - P_e - P_c. \qquad (4\text{-}24)$$

Note that the integration of a gaussian distribution from minus infinity to infinity is equal to one. The relationship is expressed as

$$1 = \frac{1}{\sqrt{2\pi}\,\sigma}\int_{-\infty}^{\infty} e^{-(r-E_s)^2/2\sigma^2}dr. \qquad (4\text{-}25)$$

Using (4-22), (4-24), and (4-25), we get

$$P_E = \frac{1}{\sqrt{2\pi}\,\sigma}\int_{-\infty}^{\infty} e^{-(r-E_s)^2/2\sigma^2}[1-\{1-Q[(r/d-E_s/2)/\sigma]\}^{31}]dr - P_e. \qquad (4\text{-}26)$$

For a very small P_E, the two-term binomial expansion in (4-13) can be used to approximate (4-26) as

$$P_E = \frac{31}{\sqrt{2\pi}\,\sigma}\int_{-\infty}^{\infty} e^{-(r-E_s)^2/2\sigma^2}Q(r/d-E_s/2)/\sigma]dr - P_e. \qquad (4\text{-}27)$$

P_e is numerically computed using (4-23), and P_E is numerically computed using (4-26) for high P_E values and (4-27) for low P_E values. With the obtained data, P_E vs. P_e for constant values of E_s/N_o are plotted in figure 4.5. The loci of constant t are also shown. Superimposing the P_w curves from figure 3.1 on the above curves, a P_w vs. SNR plot, which enables us to predict the detection system performance, is generated.

Figure 4.5 shows that the ratio setting of d=1.Ø6 yields low word error probabilities. We find that the ratio setting is the optimum setting for all values of E_s/N_o shown in the P_E vs P_e graph. If d is varied over the range $1.Ø3 < d < 1.1Ø$, then the effect on the word error probability will be minimal.

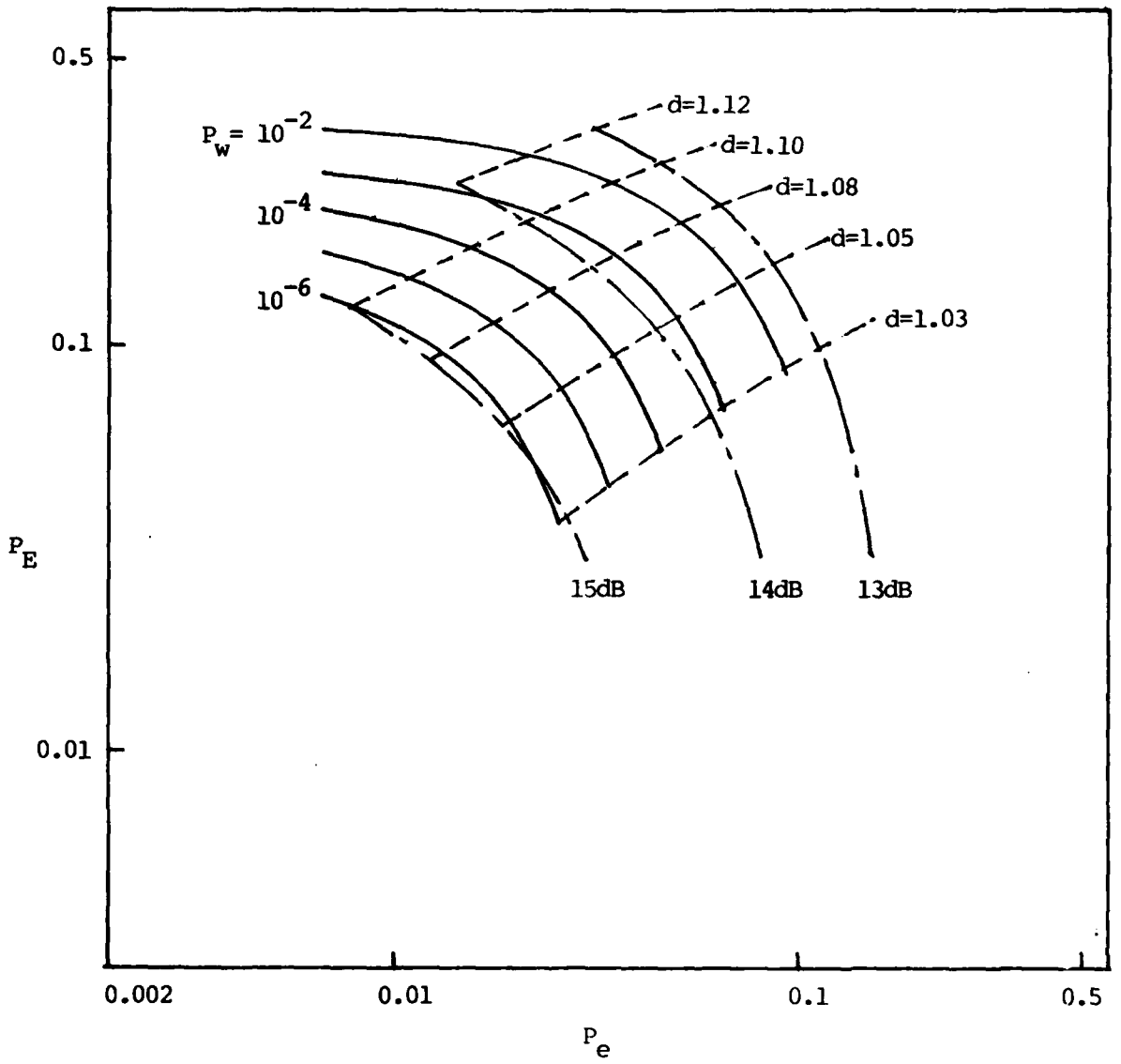

Figure 4.5. Ratio rule orthogonal signalling performance curves.

4.2.2 Analysis of the Ratio Rule Performance for Antipodal Signalling

For the present analysis of the ratio rule performance, (4-16) and (4-17) hold true.

The probability analysis for antipodal signalling is essentially the same as the analysis for orthogonal signalling, but the statistical mean value for r_i (for i=1,2,...,31) is zero for antipodal signalling. Without retracing the derivations we will simply state the necessary relationships for the performance analysis as follows

$$P_C = \frac{1}{\sqrt{2\pi}\,\sigma}\int_{-\infty}^{\infty} e^{-(r-E_s)^2/2\sigma^2}\{1-Q[r/d\sigma]\}^{31}dr \qquad (4\text{-}28)$$

$$P_e = \frac{31}{\sqrt{2\pi}\,\sigma}\int_{-\infty}^{\infty} e^{-r^2/2\sigma^2}\{1-Q[r/d\sigma]\}^{30}\{1-Q[(r/d-E_s)1/\sigma]\}dr \qquad (4\text{-}29)$$

$$P_E = \frac{1}{\sqrt{2\pi}\,\sigma}\int_{-\infty}^{\infty} e^{-(r-E_s)^2/2\sigma^2}[1-\{1-Q[r/d\sigma]\}^{31}]dr - P_e. \qquad (4\text{-}30)$$

Using the definition in (4-16), (4-29) and (4-30) can be numerically computed. By plotting the curves as was done for orthogonal signalling we are able to predict the probability of a word error.

The curves derived from the numerical analysis of (4-29) and (4-30) are shown in fig. 4.6. We see that the ratio setting of d=1.18 yields low word error probabilities. The ratio setting is optimum for all values of E_s/N_o shown in the P_E vs. P_e graph. If d is varied over the range $1.11 < d < 1.28$, then the effect on the word error probability will be minimal.

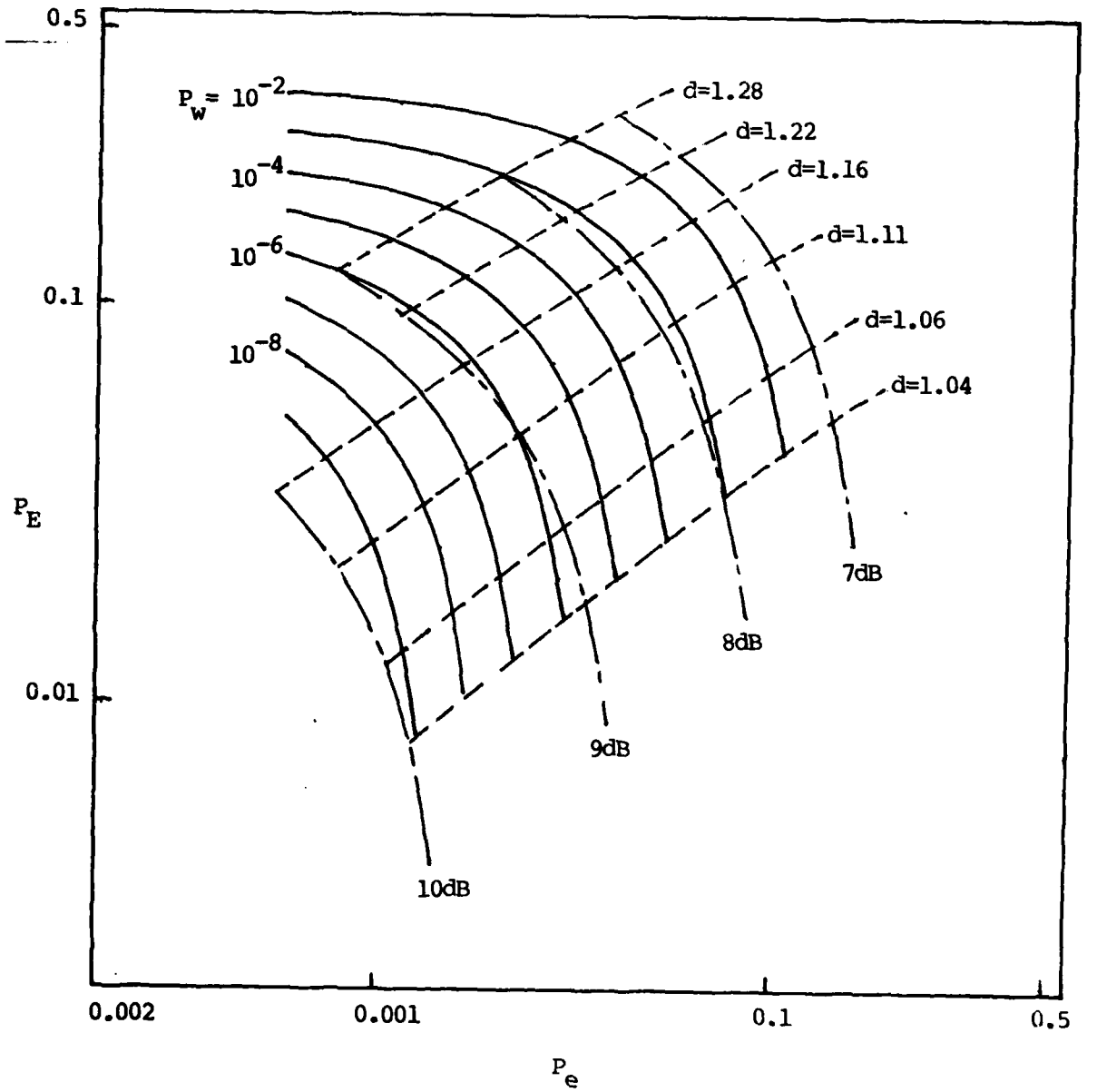

Figure 4.6. Ratio rule antipodal signalling performance curves.

4.3 Discussion of the Results of the Analog Correlation Analysis

We analyzed the performance of a detection system using the threshold rule and of a detection system using the ratio rule for orthogonal signalling and antipodal signalling.

Comparing the performance results of the threshold rule and of the ratio rule, we find that the optimum ratio setting for the ratio rule is relatively invariant with respect to changes in SNR, whereas we see the optimum threshold setting for the threshold rule varying with changes in SNR. When the detection system performance for ratio rule is compared with the performance for threshold rule the ratio rule performance is slightly better. We can conclude that for the case of analog correlation, the ratio rule is better than the threshold rule.

When the detection system performance for orthogonal signalling and for antipodal signalling are compared, we find that antipodal signalling achieves the same probability of a word error as orthogonal signalling for 6 dB less than the SNR required for orthogonal signalling. Therefore, antipodal signalling proves to be better than orthogonal signalling in terms of detection system performance.

In this chapter we analyzed the detection system performance for analog correlation. As seen in fig. 4.2, the symbol detector consists of 32 correlators, each holding a reference signal corresponding to a 32-ary symbol. Each correlator produces an analog output. The correlator outputs are used by the decision logic device to make a symbol decision.

CHAPTER 5

DIGITAL SIGNAL DETECTION

This chapter investigates the detection system performance analysis for the case of digital correlation. For this case, the received signals are digitized on a chip-by-chip basis.

The chief advantage to the use of digitization is that it simplifies the hardware design and implementation. But digitization carries the penalty of a small performance degradation when compared to the system performance for analog signal processing.

A block diagram of the digital detection system is shown in fig. 5.1. For the digital detection system, a chip detector precedes the bank of digital correlators. There are 32 digital correlators, each corresponding to a 32-ary symbol.

Each symbol is represented by a code of 32 chips. An i'th correlator correlates the code from the chip detector with its reference code c_i and generates the quantized correlator output r_i, where r_i=-32,30,...,0,...,30,32 and i=0,1,...,31. Upon completion of the digital correlation process, the decision logic device takes the symbol correlator outputs and decides upon a symbol from the symbol set

$$U = \{\mu_0, \mu_1, \ldots, \mu_{31}, \text{erasure}\} \qquad (5\text{-}1)$$

using either the threshold rule or the ratio rule. The symbol decision is

sent to the Reed-Solomon decoder. The decoder takes the 31 symbol decisions comprising an R-S (31,15) code and decodes it into 15 information symbols.

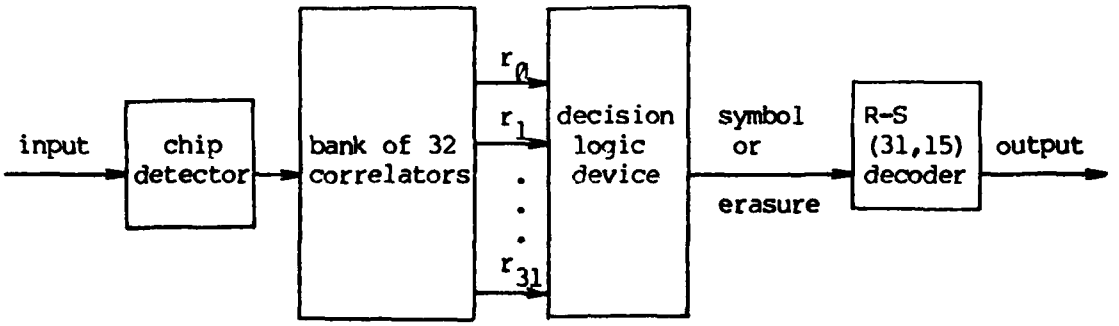

Figure 5.1. Diagram of the digital detection system.

Hard decisions are made by the chip detector for each received chip signal. For simplicity of analysis, we assume that each hard decision yields a value of 1 or -1, depending upon the received chip signal.

Important assumptions are made about the chips making up a symbol. The 32 chips representing the i'th symbol are polar (1,-1) digits comprising a code word c_i, where $i=0,1,\ldots,31$. Furthermore, each code word c_i has orthogonal correlation properties. We assume that when a code word is correlated with itself, there are 32 chip agreements, and when a code word c_i is correlated with c_j (for $i \neq j$), there are 16 chip agreements and 16 chip disagreements. Since for PSK each chip agreement yields 1 and each chip disagreement yields -1, correlation of c_i with itself will yield an output of 32, and correlation of c_i with c_j (for $i \neq j$) will yield an output of 0.

The decision rules developed and analyzed for analog correlation in the last chapter will be analyzed for digital correlation in this chapter. The results of the digital correlation analysis will be compared with the results of the analog correlation analysis. Because of the quantization of signals in digital correlation, we expect some level of performance degradation when compared to the system performance achieved with analog correlation.

For this chapter, we considered antipodal signalling for modulating the chips. For orthogonal signalling, we add 3 dB to each constant SNR curve.

5.1 Analysis of Digital Signal Detection

Assuming that the chips comprising a code word are transmitted using antipodal signalling and the energy in the received signal is E_s, the probability of a chip error occurring at the chip detector is

$$P_{ce} = Q\left[\sqrt{2E_s/32N_o}\right] \qquad (5\text{-}2)$$

where $E_s/32$ is the energy of each PSK modulated chip and $N_o/2$ is the power spectral density of white noise. The relationship in (5-2) is used to formulate various probability relationships necessary for performance analysis of digital signal detection. We study the four basic probability analyses fundamental to our performance analysis.

Case 1: The probability that $r_i \geq t$ for $i \neq \emptyset$.

There are 32 digital correlators in the digital detection system. Since it was assumed that $x_\emptyset(t)$ is the transmitted signal the correlator outputs are seperated into two cases: $r_\emptyset$ and r_i (for i=1,2,...,31). Because we are dealing with orthogonal codes, for noiseless channel, the correlator outputs have the values

$$r_\emptyset = 32 \qquad (5\text{-}3a)$$

$$r_i = \emptyset \qquad i=1,2,\ldots,31. \qquad (5\text{-}3b)$$

We will refer to r_i for which i=1,2,...,31 as r_i, and r_i for which $i=\emptyset$ as $r_\emptyset$ throughout the report.

The range of r_i depends on the $\emptyset$ to 32 possible chip errors in a 32-chip sequence. Figure 5.2 illustrates all possible values of r_i given k, the number of chip errors.

We explain fig. 5.2 by using examples. With no error, r_i is $\emptyset$ because it is the sum of 16 1's (sign agreements) and 16 -1's (sign disagreements) in the chip-by-chip correlation of c_i and c_j, where $i \neq j$. With one error, r_i can be -2 when it is the sum of 15 1's and 17 -1's, or r_i can be 2 when it is the sum of 17 1's and 15 -1's. We can do the same calculations for other k values (the number of chip errors) and verify the results in fig. 5.2.

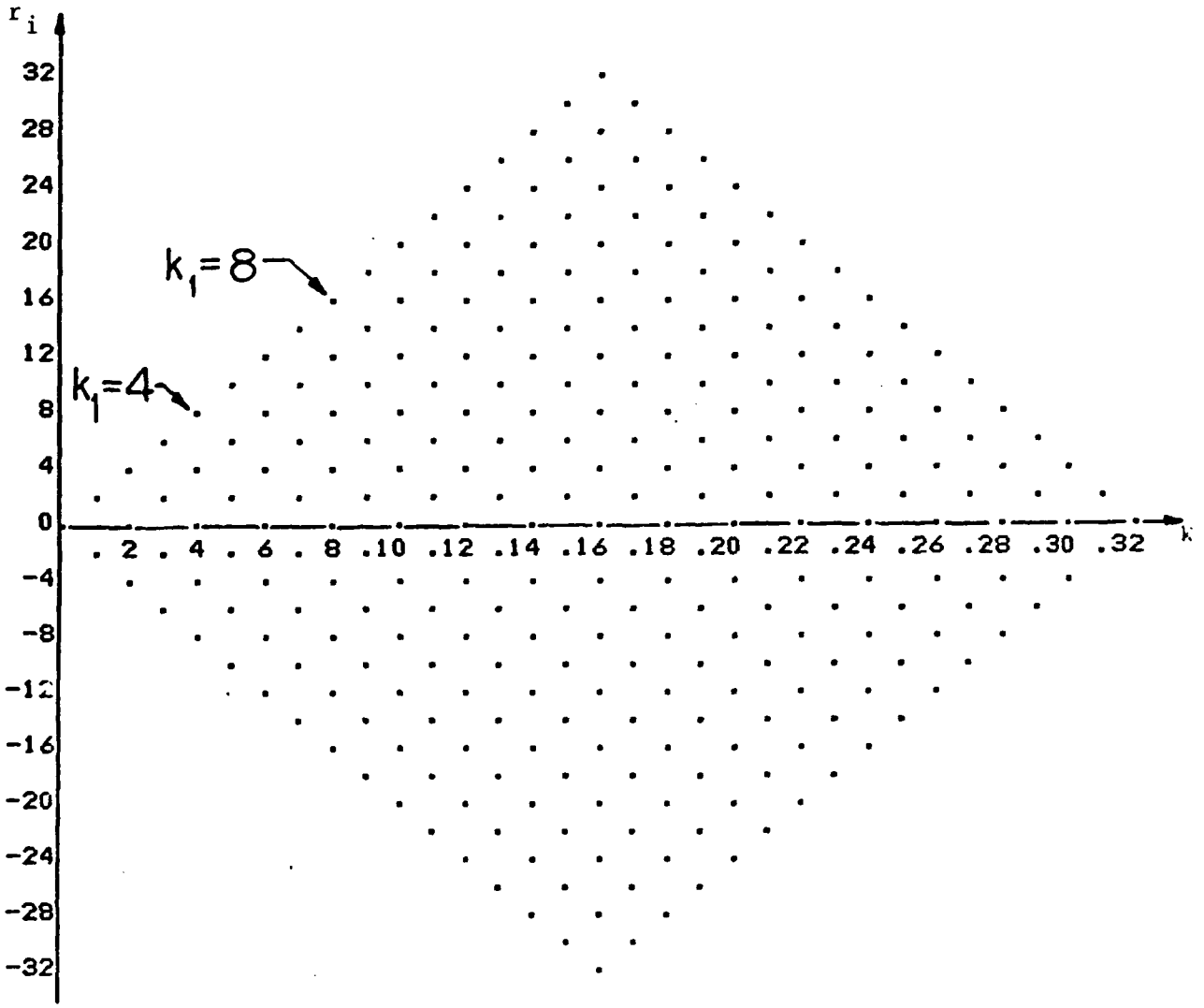

Figure 5.2. Possible values of r_i as a function of k.

The probability that r_i is greater than or equal to t can be expressed as

$$P(r_i \geq t) = \sum_{k=\lceil t/2 \rceil}^{\lfloor 32-t/2 \rfloor} P[r_i \geq t | k] P(k) \qquad (5\text{-}4)$$

where $\lfloor 32-t/2 \rfloor$ is the floor of 32-t/2, or the greatest integer less than or equal to 32-t/2, and $\lceil t/2 \rceil$ is the ceiling of t/2, or the least integer greater than or equal to t/2. The probability is equivalent to the sum of the probabilities of all the coordinate points located at or above the line r_i=t.

P(k) is the probability of k errors occurring in a 32-chip code word. The k errors in a chip sequence can arrange themselves in many different ways, requiring a combinatorial analysis. P(k) is expressed as

$$P(k) = \binom{32}{k} P_{ce}(1-P_{ce})^{32-k} \qquad (5\text{-}5)$$

where P_{ce} is the probability of a chip error as defined in (5-2), and $(1-P_{ce})$ is the probability of an error-free chip. Combining (5-4) and (5-5), we obtain

$$P[r_i \geq t] = \sum_{k=\lceil t/2 \rceil}^{\lfloor 32-t/2 \rfloor} P[r_i \geq t | k] \binom{32}{k} P_{ce}(1-P_{ce})^{32-k}. \qquad (5\text{-}6)$$

The number of chip errors k can be defined as

$$k = k_1 + k_2 \qquad (5\text{-}7)$$

where k_1 is the number of chip errors which cause a positive contribution to the correlator output and k_2 is the number of chip errors which cause a negative contribution to the correlator output. The reader is referred to fig. 5.2 to note that chip errors cause only even integral contributions to the symbol correlator outputs. Using (5-7), (5-6) is expanded to get

$$P[r_i \geq t] = \sum_{k=\lceil t/2 \rceil}^{16} \sum_{k_1=\lceil (t+2k)/4 \rceil}^{k} \binom{16}{k_1}\binom{16}{k-k_1} P_{ce}(1-P_{ce})^{32-k}$$

$$+ \sum_{k=\lceil t/2 \rceil}^{\lfloor 32-t/2 \rfloor} \sum_{k_1=\lceil (t+2k)/4 \rceil}^{16} \binom{16}{k_1}\binom{16}{k-k_1} P_{ce}(1-P_{ce})^{32-k}. \qquad (5\text{-}8)$$

Equation (5-8) was derived by summing the probabilities of the coordinate points occurring at or above the horizontal t line along the vertical constant k lines. This approach required us to break the expression into two terms. A more simplified equation was later derived when the probabilities of the points occurring at or above the horizontal t line along the diagonal constant k_1 lines were summed. The expression derived is

$$P[r_i \geq t] = \sum_{k_1=\lceil t/2 \rceil}^{16} \sum_{k=k1}^{\lceil 2k_1 - t/2 \rceil} \binom{16}{k_1}\binom{16}{k-k_1} P_{ce}(1-P_{ce})^{32-k}. \qquad (5\text{-}9)$$

This is the final expression describing the probability that r_i is greater than or equal to t. The two independent variables in the equation are t and P_{ce}.

Case 2: The situation in which $r_{\emptyset} \geq t$.

We would like to find the probability that $r_{\emptyset}$ is greater than or equal to t. Note that $r_{\emptyset}$ is 32 when there exist no chip errors. But with each chip error, the $r_{\emptyset}$ value is decremented by 2. The maximum allowable number of chip errors in a 32-chip code is 32, in which case the $r_{\emptyset}$ value is -32. The probability that $r_{\emptyset}$ is greater than or equal to t is written as

$$P[r_{\emptyset} \geq t] = \sum_{k=\emptyset}^{\lfloor 16-t/2 \rfloor} \binom{32}{k} P_{ce}(1-P_{ce})^{32-k}. \qquad (5\text{-}1\emptyset)$$

The two independent variables in (5-1Ø) are t and P_{ce}.

Case 3: The case in which $r_i = 2I$.

Referring to figure 5.2, the probability that r_i equals an even integral value 2I is the sum of the probabilities of the points occurring coincident to the horizontal line $r_i = 2I$. Along such a line k and k_1 are related as $4k_1 - 2k = 2I$. The probability is expressed as

$$P[r_i = 2I] = \sum_{k_1=I}^{16} \binom{16}{k_1} \binom{16}{k_1 - I} (P_{ce})^{2k_1 - I} (1-P_{ce})^{32-2k_1+I} \qquad (5\text{-}11)$$

Case 4: The case in which $r_\emptyset = 2I$.

Finding the probability that $r_\emptyset$ equals an even integral value 2I is rather straightforward. Note that the $r_\emptyset$ value in the absence of chip errors is 32; $r_\emptyset$ and k are related as

$$k = (32-r_\emptyset)/2. \tag{5-12a}$$

When 2I is substituted for $r_\emptyset$ in (5-12a) we get

$$k = 16 - I. \tag{5-12b}$$

The probability that $r_\emptyset$ equals 2I is

$$P[r_\emptyset=2I] = \binom{32}{k} (P_{ce})^k (1-P_{ce})^{32-k}. \tag{5-13a}$$

But when 16-I is substituted for k we get

$$P[r_\emptyset=2I] = \binom{32}{16-I} (P_{ce})^{16-I} (1-P_{ce})^{16+I}. \tag{5-13b}$$

Having obtained the expressions for $P[r_i \geq t]$, $P[r_\emptyset \geq t]$, $P[r_i=2I]$, and $P[r_\emptyset=2I]$ we can proceed to evaluate the error probabilities and erasure probabilities associated with the threshold rule and the ratio rule.

5.2 Threshold Rule Analysis

For a correct symbol decision to occur, $r_\emptyset$ must be greater than or equal to the threshold setting t, and all r_i (for i=1,2,....,31) must be less than $r_\emptyset$. Since the correlator outputs are even integers, they can be represented as 2I, I being any integer. The expression for the probability of a correct decision is given by

$$P_c = \sum_{I=\lceil t/2 \rceil}^{16} P(r_\emptyset = 2I)\,[1-P(r_i \geq 2I)]^{31}. \qquad (5\text{-}14)$$

For an error to occur, one of the r_i correlator outputs must be the largest correlator output and must equal or exceed the threshold t, and the rest of the correlator outputs, including $r_\emptyset$, must be less than the largest correlator output value. The expression for the probability of an error is given by

$$P_e = 31 \sum_{I=\lceil t/2 \rceil}^{16} P(r_i = 2I)\,[P(r_i < 2I)]^{30} P(r_\emptyset < 2I). \qquad (5\text{-}15a)$$

Putting this in terms of the previously defined terms, we obtain

$$P_e = 31 \sum_{I=\lceil t/2 \rceil}^{16} P(r_i = 2I)\,[1-P(r_i \geq 2I)]^{30}\,[1-P(r_\emptyset \geq 2I)]. \qquad (5\text{-}15b)$$

The probability of an erasure is formulated by simply taking the probability of a correct decision and the probability of an error, which are defined in (5-14) and (5-15b), and subtracting them from 1 as follows

$$P_E = 1 - P_c - P_e \qquad (5\text{-}16)$$

P_E and P_e are numerically computed and the curves are plotted to predict the digital detection system performance using the threshold rule. The performance curves found in fig. 5.3 show that the threshold should be set at t=12 to yield the lowest word error probability. The threshold setting can be varied in the range of $10 < t < 14$ without substantially affecting the probability of a word error.

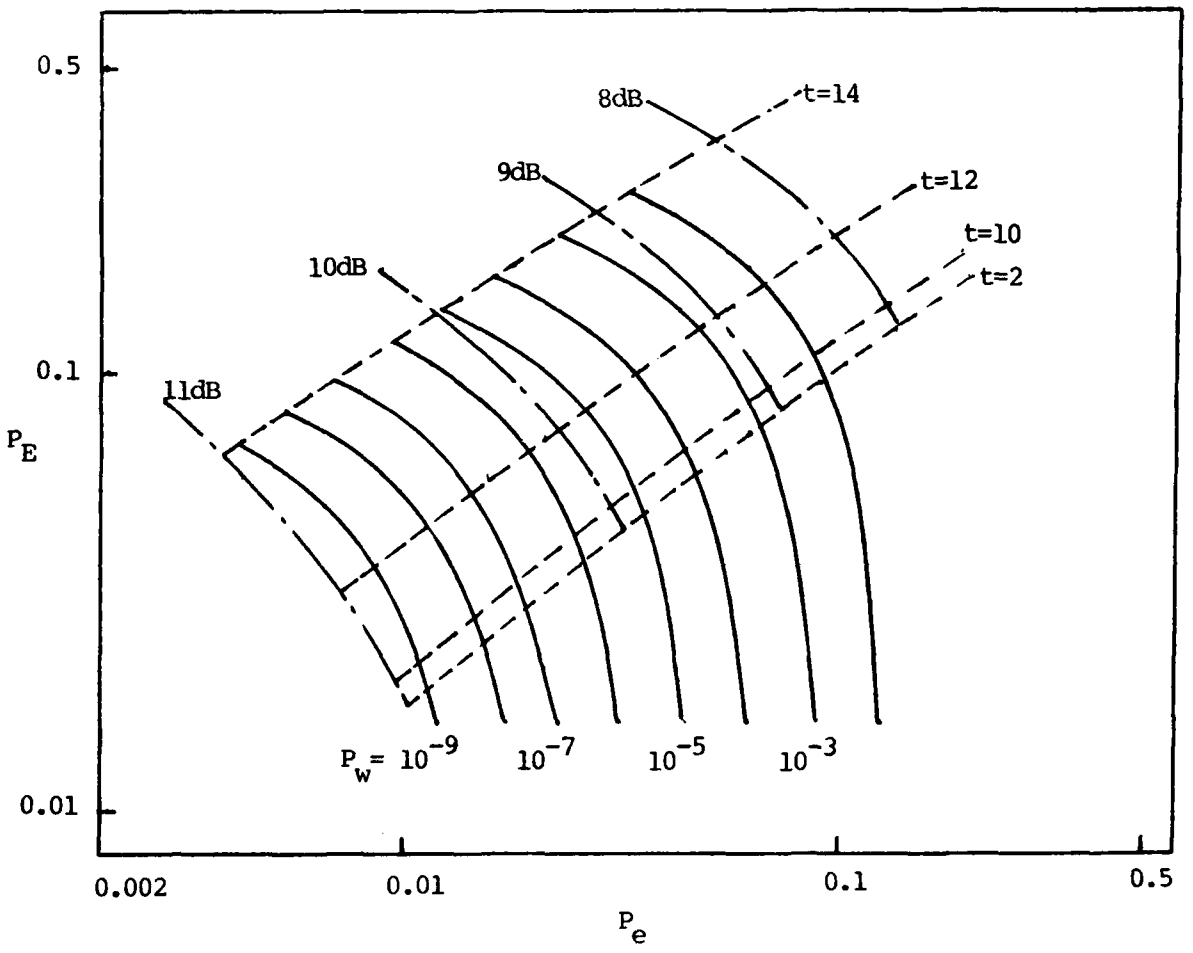

Figure 5.3. Threshold rule digital correlation performance curves.

5.3 Ratio Rule Analysis

For a correct symbol decision to occur, $r_\emptyset$ must be greater than or equal to d times the largest r_i value, where d is the ratio setting which can take on any real value that is greater than 1. When errors are introduced, the $r_\emptyset$ and r_i values must be even integers ranging from -32 to 32. For the ratio rule, we approximate our analysis by assuming that the probability of 17 or more chip errors occurring in a code of 32 chips is insignificant. Therefore, we restrict our analysis to the case where only 16 or fewer chip errors occur. We make the above restriction because the ratio rule performance analysis becomes complicated when negative $r_\emptyset$ values are introduced. We express the probability of a correct decision as

$$P_c = \sum_{I=\emptyset}^{16} P(r_\emptyset=2I)\,[1-P(r_i \geq d(2I))]^{31}. \qquad (5\text{-}17)$$

For an error to occur, one of the r_i correlator outputs must be the largest correlator output which equals or exceeds a value that is d times the value of the second largest correlator output, where d is the variable ratio setting which takes on a real value that is greater than 1. The probability of an error can be expressed as

$$P_e = 31 \sum_{I=\emptyset}^{16} P(r_i=2I)\,[1-P(r_i \geq d(2I))]^{30}\,[1-P(r_\emptyset \geq d(2I))] \qquad (5\text{-}18)$$

The analysis of the probability of an erasure is not easy because it involves many different cases of an erasure, so we define the probability of an erasure as 1 minus the sum of the probability of a correct decision and the

probability of an error, or

$$P_E = 1 - P_c - P_e. \qquad (5\text{-}19)$$

We can numerically compute the P_E and P_e equations and plot the curves to predict the digital detection system performance when the ratio rule is used. The performance curves are shown in fig. 5.4. The optimum value of d is 1.25 for the SNR range of 8 dB to 11 dB. It is not critical to maintain this value of d because low word error probabilities can be obtained for a broad range of values of d.

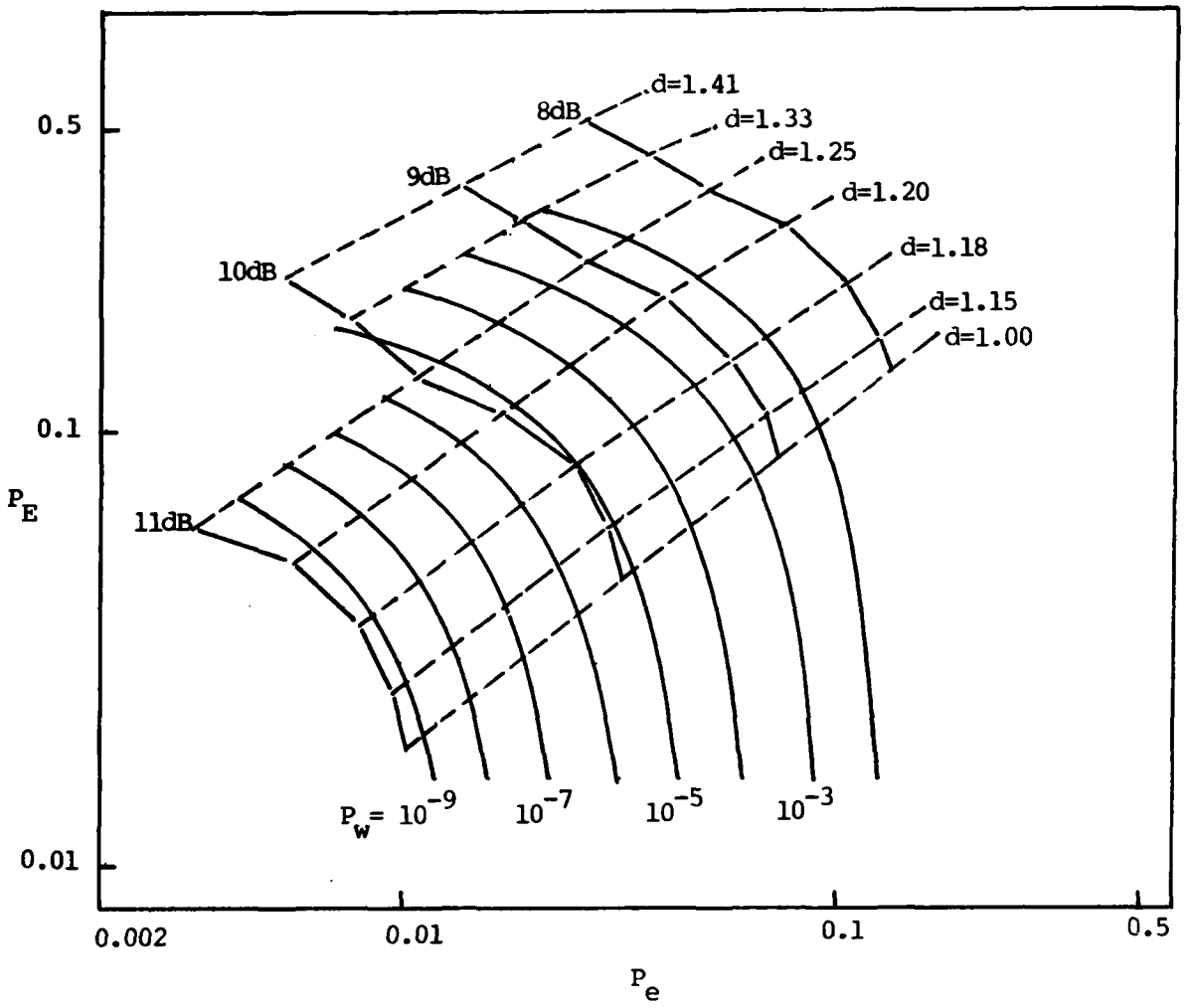

Figure 5.4. Ratio rule digital correlation performance curves.

5.4 Discussion of the Results of the Digital Correlation Analysis

Comparing the performance results of the two decision rules, we find the optimum ratio setting for the ratio rule and the optimum threshold setting for the threshold rule are relatively invariant with respect to changes in E_s/N_o. This was not the case for the threshold rule of analog correlation. For the digital correlation case studied in this chapter we find no distinct advantage of one decision rule over the other.

Recall that for the digital correlation case the chip detector outputs are quantized. This means that the correlation values are quantized into even integral values ranging from -32 to 32. The quantization of the correlator outputs also quantizes the values that the threshold setting of the threshold rule can take on. The threshold setting can have an even integral value which ranges from 0 to 32. However, the values that the ratio setting for the ratio rule can have due to quantization are not easy to see, but we do find discrete ratio settings which do affect the system performance. For example, the system performance is not affected unless the ratio setting makes a transition through any of the following values: 1.0,1.15,1.18,1.20,1.25,1.33,1.41. Of course, d can have higher values, but they were not observed because they fell out of the range of d values of our interest.

There is a noticeable performance degradation when digital correlation is used instead of the analog correlation. In terms of SNR, we see less than 1 dB performance degradation when digital correlation is used. The small

degradation in the system performance is acceptable when we consider that the design and implementation of the digital detector is simpler than the analog detector.

CHAPTER 6

MONTE CARLO SIMULATION

In Chapter 5 the detection system performance for various cases was analyzed. The derived equations were numerically analyzed, and the data obtained were used to plot the performance curves. In this chapter we try to simulate the operation of the digital detection system and obtain performance data which can be compared with the data derived from the analysis. The Monte Carlo simulation method is used to process signals which are noise corrupted. Antipodal signalling was considered. The decision rule used was the threshold rule.

6.1 The Simulation Program

The digital detection system shown in fig. 5.1 was chosen for the Monte Carlo simulation. The operation of the chip detector, the bank of 32 correlators, and the decision logic device using the threshold rule are modeled by the simulation program.

The system uses 32-chip codes which have orthogonal correlation properties. The maximal-length sequences and the Welti codes are investigated for use as the operating codes. The performances for the two cases are compared to each other and to the performance predicted by the analysis in Chapter 5. We will later see that the simulation using the modified maximal-length sequences and the simulation using the Welti codes yield

identical performance results, but the simulation results do not sufficiently agree with the results obtained from the analysis.

The simulation repetitively processes $x_0(t)$ which is corrupted with random noise; 10,000 samples of 32 detected chips are collected, and the symbol decisions are evaluated to find the relative frequencies of symbol erasures and symbol errors.

6.1.1 Chip Detector

The operation of the chip detector is modeled using the random number generator. We use the relationship

$$P_{ce} = Q\left[\sqrt{2E_s/32N_o}\right] \qquad (6\text{-}1)$$

to relate the given SNR to P_{ce}. The random number generator is used to generate independent chip errors at the relative frequency that approaches the probability of a chip error for a large number of chip samples. For 10,000 samples of a 32-chip code, it is typical to find the relative frequency of chip errors accurate to 3 significant digits when compared to the given probability of a chip error.

6.1.2 Digital Correlators

An i'th digital correlator takes the 32 detected chips and correlates it with the reference code c_i. The correlation output r_i can take on an even integral value ranging from -32 to 32. As stated earlier, $x_\emptyset$ is assumed to be transmitted without any loss of generality. Since we are dealing with orthogonal codes, under the noiseless condition, we should find that

$$r_\emptyset = \langle c_\emptyset, c_\emptyset \rangle = 32$$
$$r_1 = \langle c_\emptyset, c_1 \rangle = \emptyset$$
$$r_2 = \langle c_\emptyset, c_2 \rangle = \emptyset$$
$$\vdots \qquad\qquad \vdots$$
$$r_{31} = \langle c_\emptyset, c_{31} \rangle = \emptyset$$

6.1.3 Decision Logic Device

The decision logic device takes the 32 correlation outputs and makes a symbol decision using the threshold rule. The threshold rule makes a symbol decision if the threshold criterion is met, but if the threshold criterion is not met then an erasure is declared. An erasure is declared when the received signal has unacceptably degraded in signal quality due to the noise present in the transmission medium.

The threshold rule is implemented in the simulation as follows: If the largest correlator output equals or exceeds the threshold, then declare the symbol corresponding to the correlator as the received symbol. If either the largest correlator output does not exceed the threshold or if we have a tie, then declare an erasure.

Since we know which symbol is sent (we assumed that μ_0 is sent throughout the report), we can take a symbol decision and determine if the decision was correct or if it was in error. By counting the occurrences of errors and erasures, we are able to find the relative frequencies of errors and erasures.

6.2 Codes

Codes are a set of code words used to generate signals. For the spread spectrum communication system that we examined, each 32-ary symbol is represented by a code word of length 32. Although the actual codes used are psuedo-orthogonal, for simplicity of analysis, we assume codes with orthogonal correlation properties.

The two codes investigated are the maximal-length sequences and the Welti codes. The codes were used to simulate the system operation and obtain the performance data. The data were used to plot the performance curves.

6.2.1 Maximal-Length Sequences

In this section, a methodology for producing maximal-length sequences of length 31, each having the periodic correlation function

$$\theta(\tau) = \begin{cases} 31 & \tau=\emptyset \\ -1 & \tau\neq\emptyset \end{cases} \qquad (6\text{-}2)$$

is discussed. The maximal-length sequences are then modified to yield codes of 32 chips having the orthogonal correlation properties. If the reader is interested in a general discussion of binary maximal-length sequences, then the reader is referred to Bhargava, Haccoun, Matyas, and Nuspl [7].

Maximal-length sequences, or m-sequences, can be generated by a linear feedback shift-register generator (LFSRG). Given an m-stage LFSRG, a set of maximal-length sequences of length N can be generated, where

$$N = 2^m - 1. \qquad (6\text{-}3)$$

Although we would like to get 32-ary code words, (6-3) tells us that this is not possible. We can take the next best choice of generating 31-ary code words. As it turns out, it is possible to modify the maximal-length sequences so that we can obtain 32-ary code words with orthogonal correlation properties.

To get a set of maximal-length sequences of length 31, a 5-stage LFSRG must be used. We use the equation,

$$h(x) = h_\emptyset + h_1x + h_2x^2 + h_3x^3 + h_4x^4 + h_5x^5 \qquad (6\text{-}4a)$$

where h(x) is the associated polynomial of the shift register with feedback coefficients ($h_0, h_1, \ldots, h_5$). If the feedback coefficients are defined as $h_0=1$, $h_1=0$, $h_2=1$, $h_3=0$, $h_4=0$, $h_5=1$, corresponding to the entries in the connection vector (101001) for a 5-stage shift register, the equation can be simplified as

$$h(x) = 1 + x^2 + x^5. \qquad (6\text{-}4b)$$

The 5-stage LFSRG modeled by (6-4b) is shown in figure 6.1. The initial state is assumed to be (10000), but any set of 5 binary digits that is not (00000) can be used. The output from the last stage of the shift register is used to sequentially extract maximal-length sequences.

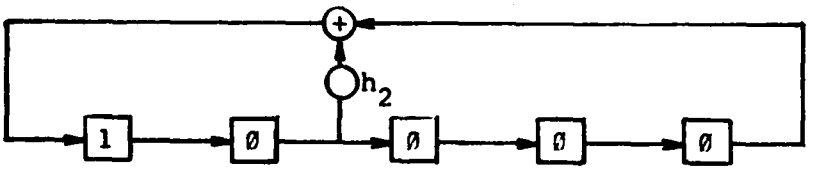

Figure 6.1. 5-Stage Linear Feedback Shift-Register Generator.

A sample maximal-length sequence is found in fig. 6.2a. A second maximal-length sequence is found in fig. 6.2b. Each maximal-length sequence generated by an LFSRG is a cyclical shift of another. In order to have a binary (+1,-1) chip sequence, we convert all 0's into -1's. The binary (1,0) sequence in fig. 6.2a becomes the binary (+1,-1) sequence in fig. 6.2c, and the binary (1,0) sequence in fig. 6.2b becomes the binary (+1,-1) sequence in

fig. 6.2d. The periodic correlation function for the binary (+1,-1) sequence is given by

$$\theta(\tau) = \begin{cases} 31 & \tau=\emptyset \\ -1 & \tau\neq\emptyset \end{cases} \qquad (6\text{-}5)$$

---

0 0 0 1 0 1 0 1 1 1 0 1 1 0 0 0 1 1 1 1 1 0 0 1 1 0 1 0 0 1 0

a. A sample maximal-length sequence of length 31.

0 0 1 0 1 0 1 1 1 0 1 1 0 0 0 1 1 1 1 1 1 0 0 1 1 0 1 0 0 1 0 0

b. Another maximal-length sequence of length 31.

-1-1-1 1-1 1-1 1 1 1-1 1 1-1-1-1 1 1 1 1 1-1-1 1 1-1 1-1-1 1-1

c. A binary (+1,-1) sequence obtained from the sequence in fig. 6.2a.

-1-1 1-1 1-1 1 1 1-1 1 1-1-1-1 1 1 1 1 1-1-1 1 1-1 1-1-1 1-1-1

d. A binary (+1,-1) sequence obtained from the sequence in fig. 6.2b.

1 1-1-1-1-1-1 1 1-1-1 1-1 1 1-1 1 1 1 1-1 1-1 1-1-1-1 1-1-1 1

e. A sequence of chip correlation outputs.

Figure 6.2. Maximal-Length Sequences of Length 31.

Thirty-one maximal-length sequences are shown in fig. 6.3a. Each sequence can be used to represent a 31-ary code word. To generate 32-ary codes with orthogonal correlation properties, we append the digit -1 to each

of the 31 sequences, and we add the 32nd sequence, which consists of 32 1's, to the set of 31 sequences. The 32-ary orthogonal codes are illustrated in fig. 6.3b. The code words in fig. 6.3b have orthogonal correlation properties as follows:

a. When a code word c_i is correlated with itself, we get $r_i = 32$, where r_i is the correlation output of the i'th correlator.

b. When a code word c_i is correlated with a code word c_j (where $i \neq j$), we get $r_i = 0$.

```
-1-1-1 1-1 1-1 1 1 1-1 1 1-1-1-1 1 1 1 1 1-1-1 1 1-1 1-1-1 1-1
-1-1 1-1 1-1 1 1 1-1 1 1-1-1-1 1 1 1 1 1-1-1 1 1-1 1-1-1 1-1-1
      .                          .                       .
      .                          .                       .
      .                          .                       .
-1-1-1-1 1-1 1-1 1 1 1-1 1 1-1-1-1 1 1 1 1 1-1-1 1 1-1 1-1-1 1
```

a. Maximal-length sequences of length 31.

```
-1-1-1 1-1 1-1 1 1 1-1 1 1-1-1-1 1 1 1 1 1-1-1 1 1-1 1-1-1 1-1-1
-1-1 1-1 1-1 1 1 1-1 1 1-1-1-1 1 1 1 1 1-1-1 1 1-1 1-1-1 1-1-1-1
      .                          .                       .
      .                          .                       .
      .                          .                       .
-1-1-1-1 1-1 1-1 1 1 1-1 1 1-1-1-1 1 1 1 1 1-1-1 1 1-1 1-1-1 1-1
 1 1 1 1 1 1 1 1 1 1 1 1 1 1 1 1 1 1 1 1 1 1 1 1 1 1 1 1 1 1 1 1
```

b. 32-ary orthogonal codes.

Figure 6.3. Two Sample Codes.

The codes of length 32 in fig. 6.3b are used in the Monte Carlo simulation to produce the signals representing the 32-ary symbols. Performance data are obtained for 10,000 samples of noise corrupted signals. The performance curves derived from the data are shown in fig. 6.4.

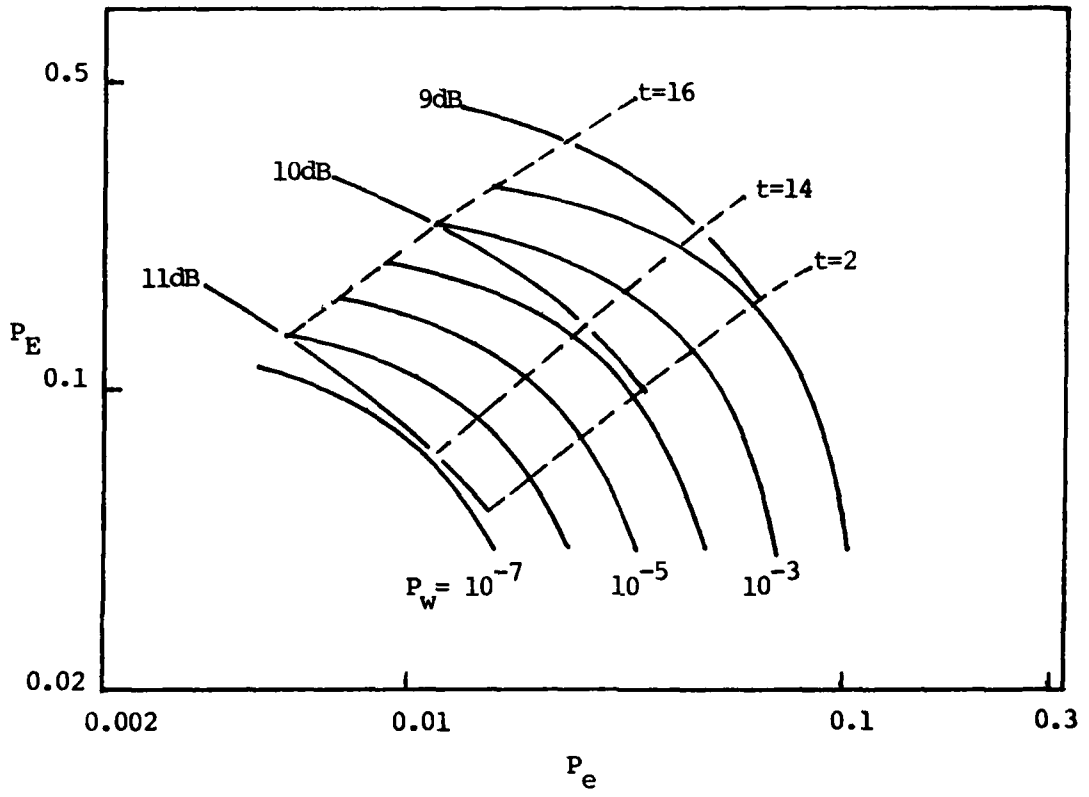

Figure 6.4. Monte Carlo simulation of digital correlation using the maximal-length sequences.

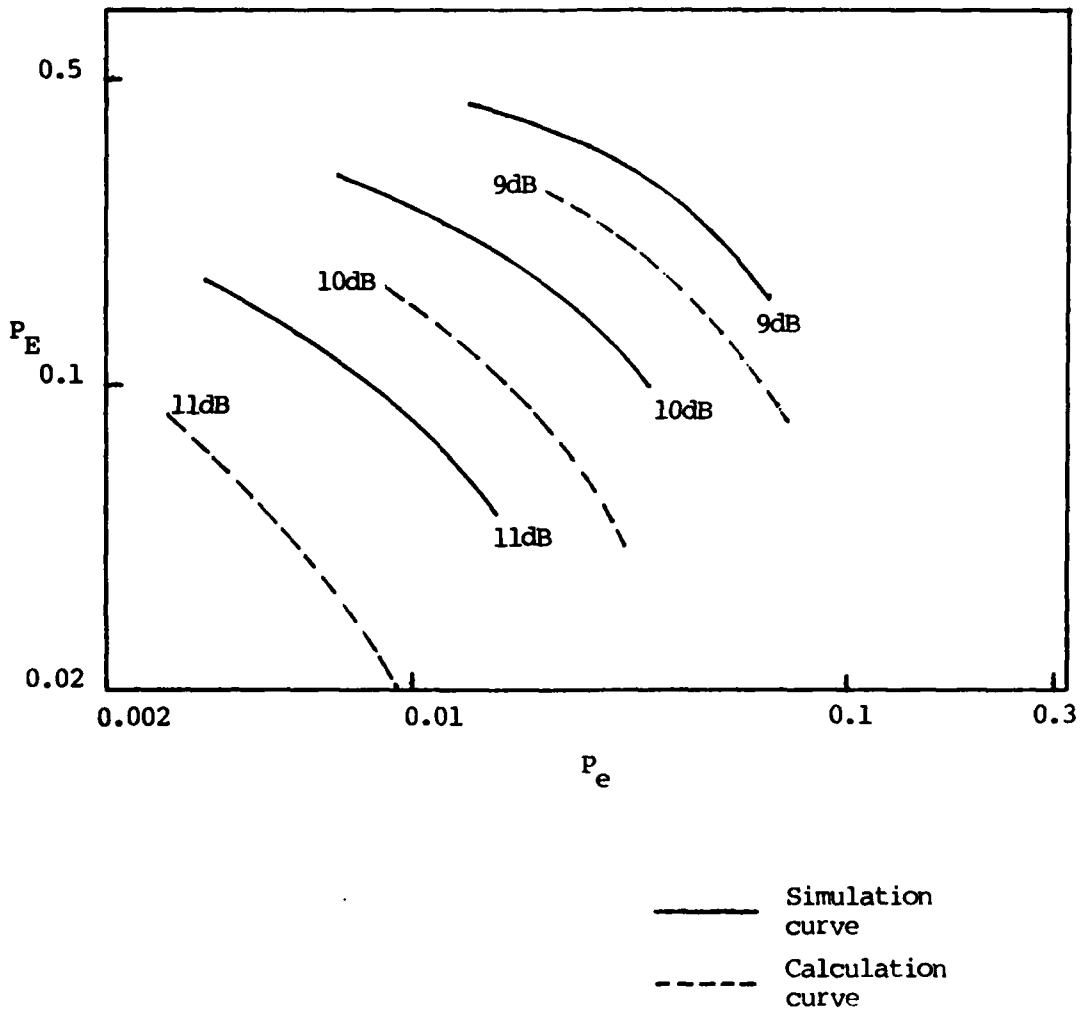

Figure 6.5. Comparison of the simulation and calculation curves.

Figure 6.5 shows that the simulation performance is worse than the performance predicted by the analysis by about -1/2 dB. Because of this difference in the performance results, we've investigated the use of another orthogonal code.

6.2.2 Welti Codes

The Welti codes [8] have orthogonal correlation properties. The codes are generated as follows: Let D_k^i represent the k'th code word of length 2^i:

$$D_k^i = (A : B) \qquad (6\text{-}6)$$

where the word is divided into sets of lengths 2^{i-1}. From this word the following are obtained:

$$D_k^{i+1} = (A : B : A : \overline{B}) \qquad (6\text{-}7)$$

$$D_{k+2^i}^{i+1} = (A : B : \overline{A} : B) \qquad (6\text{-}8)$$

where $\overline{x}$ = complement of x. For example,

$$D_0^1 = (1 \;\; 1)$$
$$D_1^1 = (1 \;\; -1)$$

Thus

$$D_0^2 = (1 \;\; 1 \;\; 1 \;\; -1)$$
$$D_2^2 = (1 \;\; 1 \;\; -1 \;\; 1)$$

$$D_1^2 = (1 \; -1 \;\; 1 \;\; 1)$$
$$D_3^2 = (1 \; -1 \; -1 \; -1)$$

and

$$D_0^3 = (1 \;\; 1 \;\; 1 \; -1 \;\; 1 \;\; 1 \; -1 \;\; 1)$$
$$D_4^3 = (1 \;\; 1 \;\; 1 \; -1 \; -1 \; -1 \;\; 1 \; -1)$$
$$D_2^3 = (1 \;\; 1 \; -1 \;\; 1 \;\; 1 \;\; 1 \;\; 1 \; -1)$$
$$D_6^3 = (1 \;\; 1 \; -1 \;\; 1 \; -1 \; -1 \; -1 \;\; 1)$$
$$D_1^3 = (1 \; -1 \;\; 1 \;\; 1 \;\; 1 \; -1 \; -1 \; -1)$$
$$D_5^3 = (1 \; -1 \;\; 1 \;\; 1 \; -1 \;\; 1 \;\; 1 \;\; 1)$$
$$D_3^3 = (1 \; -1 \; -1 \; -1 \;\; 1 \; -1 \;\; 1 \;\; 1)$$
$$D_7^3 = (1 \; -1 \; -1 \; -1 \; -1 \;\; 1 \; -1 \; -1)$$

Similarly, we can generate words of length 32. A Welti codes generator which generates the words D_0^5, D_1^5, ... , D_{32}^5 is implemented in the Monte Carlo simulation program. The set of Welti codes of length 32 is shown in figure 6.6.

Results were obtained from the Monte Carlo simulation using the Welti codes. With the obtained data, P_E vs. P_e for constant values of E_s/N_o were plotted in figure 6.7. The loci of the constant t are also shown. The P_w curves from figure 3.1 were superimposed on the above curves to generate a P_w vs. SNR plot, which enables us to predict the detection system performance.

code 0 = 1 1 1 -1 1 1 -1 1 1 1 1 -1 -1 -1 1 -1 1 1 1 -1 1 1 -1 1 -1 -1 -1 1 1 1 -1 1
code 1 = 1 -1 1 1 1 -1 -1 -1 1 -1 1 1 -1 1 1 1 1 -1 1 1 1 -1 -1 -1 -1 1 -1 -1 1 -1 -1 -1
code 2 = 1 1 -1 1 1 1 1 -1 1 1 -1 1 -1 -1 -1 1 1 1 -1 1 1 1 1 -1 -1 -1 1 -1 1 1 1 -1
code 3 = 1 -1 -1 -1 1 -1 1 1 1 -1 -1 -1 -1 1 -1 -1 1 -1 -1 -1 1 -1 1 1 -1 1 1 1 1 -1 1 1
code 4 = 1 1 1 -1 -1 -1 1 -1 1 1 1 -1 1 1 -1 1 1 1 1 -1 -1 -1 1 -1 -1 -1 -1 1 -1 -1 1 -1
code 5 = 1 -1 1 1 -1 1 1 1 1 -1 1 1 1 -1 -1 -1 1 -1 1 1 -1 1 1 1 -1 1 -1 -1 -1 1 1 1
code 6 = 1 1 -1 1 -1 -1 -1 1 1 1 -1 1 1 1 1 -1 1 1 -1 1 -1 -1 -1 1 -1 -1 1 -1 -1 -1 -1 1
code 7 = 1 -1 -1 -1 -1 1 -1 -1 1 -1 -1 -1 1 -1 1 1 1 -1 -1 -1 -1 1 -1 -1 -1 1 1 1 -1 1 -1 -1
code 8 = 1 1 1 -1 1 1 -1 1 -1 -1 -1 1 1 1 -1 1 1 1 1 -1 1 1 -1 1 1 1 1 -1 -1 -1 1 -1
code 9 = 1 -1 1 1 1 -1 -1 -1 -1 1 -1 -1 1 -1 -1 -1 1 -1 1 1 1 -1 -1 -1 1 -1 1 1 -1 1 1 1
code 10 = 1 1 -1 1 1 1 1 -1 -1 -1 1 -1 1 1 1 -1 1 1 -1 1 1 1 1 -1 1 1 -1 1 -1 -1 -1 1
code 11 = 1 -1 -1 -1 1 -1 1 1 -1 1 1 1 1 -1 1 1 1 -1 -1 -1 1 -1 1 1 1 -1 -1 -1 1 -1 -1
code 12 = 1 1 1 -1 -1 -1 1 -1 -1 -1 -1 1 -1 -1 1 -1 1 1 1 -1 -1 -1 1 -1 1 1 1 -1 1 1 -1 1
code 13 = 1 -1 1 1 -1 1 1 1 -1 1 -1 -1 -1 1 1 1 1 -1 1 1 -1 1 1 1 1 -1 1 1 1 -1 -1 -1
code 14 = 1 1 -1 1 -1 -1 -1 1 -1 -1 1 -1 -1 -1 -1 1 1 1 -1 1 -1 -1 -1 1 1 1 -1 1 1 1 1 -1
code 15 = 1 -1 -1 -1 -1 1 -1 -1 -1 1 1 1 -1 1 -1 -1 1 -1 -1 -1 -1 1 -1 -1 1 -1 -1 -1 1 -1 1 1
code 16 = 1 1 1 -1 1 1 -1 1 1 1 1 -1 -1 -1 1 -1 -1 -1 -1 1 -1 -1 1 1 1 -1 -1 -1 1 -1
code 17 = 1 -1 1 1 1 -1 -1 -1 1 -1 1 1 -1 1 1 1 -1 1 -1 -1 -1 1 1 1 1 -1 1 1 -1 1 1 1
code 18 = 1 1 -1 1 1 1 1 -1 1 1 -1 1 -1 -1 -1 1 -1 -1 1 -1 -1 -1 1 1 1 -1 1 -1 -1 -1 1
code 19 = 1 -1 -1 -1 1 -1 1 1 1 -1 -1 -1 -1 1 -1 -1 -1 1 1 1 -1 1 -1 -1 1 -1 -1 -1 -1 1 -1 -1
code 20 = 1 1 1 -1 -1 -1 1 -1 1 1 1 -1 1 1 -1 1 -1 -1 -1 1 1 1 -1 1 1 1 -1 1 1 -1 1
code 21 = 1 -1 1 1 -1 1 1 1 1 -1 1 1 1 -1 -1 -1 -1 1 -1 -1 1 -1 -1 1 -1 1 1 1 -1 -1 -1
code 22 = 1 1 -1 1 -1 -1 -1 1 1 1 -1 1 1 1 1 -1 -1 -1 1 -1 1 1 1 -1 1 1 -1 1 1 1 1 -1
code 23 = 1 -1 -1 -1 -1 1 -1 -1 1 -1 -1 -1 1 -1 1 1 -1 1 1 1 1 -1 1 1 1 -1 -1 -1 1 -1 1 1
code 24 = 1 1 1 -1 1 1 -1 1 -1 -1 -1 1 1 1 -1 1 -1 -1 -1 1 -1 -1 1 -1 -1 -1 -1 1 1 1 -1 1
code 25 = 1 -1 1 1 1 -1 -1 -1 1 -1 -1 1 1 -1 -1 -1 1 -1 -1 -1 1 1 1 -1 1 -1 -1 1 -1 -1 -1
code 26 = 1 1 -1 1 1 1 1 -1 -1 -1 1 -1 1 1 1 -1 -1 -1 1 -1 -1 -1 1 -1 1 -1 1 1 1 -1 1 -1
code 27 = 1 -1 -1 -1 1 -1 1 1 -1 1 1 1 1 -1 1 1 -1 1 1 1 -1 1 -1 -1 -1 1 1 1 1 -1 1 1
code 28 = 1 1 1 -1 -1 -1 1 -1 -1 -1 -1 1 -1 -1 1 -1 -1 -1 -1 1 1 1 -1 1 -1 -1 -1 1 -1 -1 1 -1
code 29 = 1 -1 1 1 -1 1 1 1 -1 1 -1 -1 -1 1 1 1 -1 1 -1 -1 1 -1 -1 -1 -1 1 -1 -1 -1 1 1 1
code 30 = 1 1 -1 1 -1 -1 -1 1 -1 -1 1 -1 -1 -1 -1 1 -1 -1 1 -1 1 1 1 -1 -1 -1 1 -1 -1 -1 1
code 31 = 1 -1 -1 -1 -1 1 -1 -1 -1 1 1 1 -1 1 -1 -1 -1 1 1 1 1 -1 1 1 -1 1 1 1 -1 1 -1 -1

Figure 6.6. Welti codes of length 32.

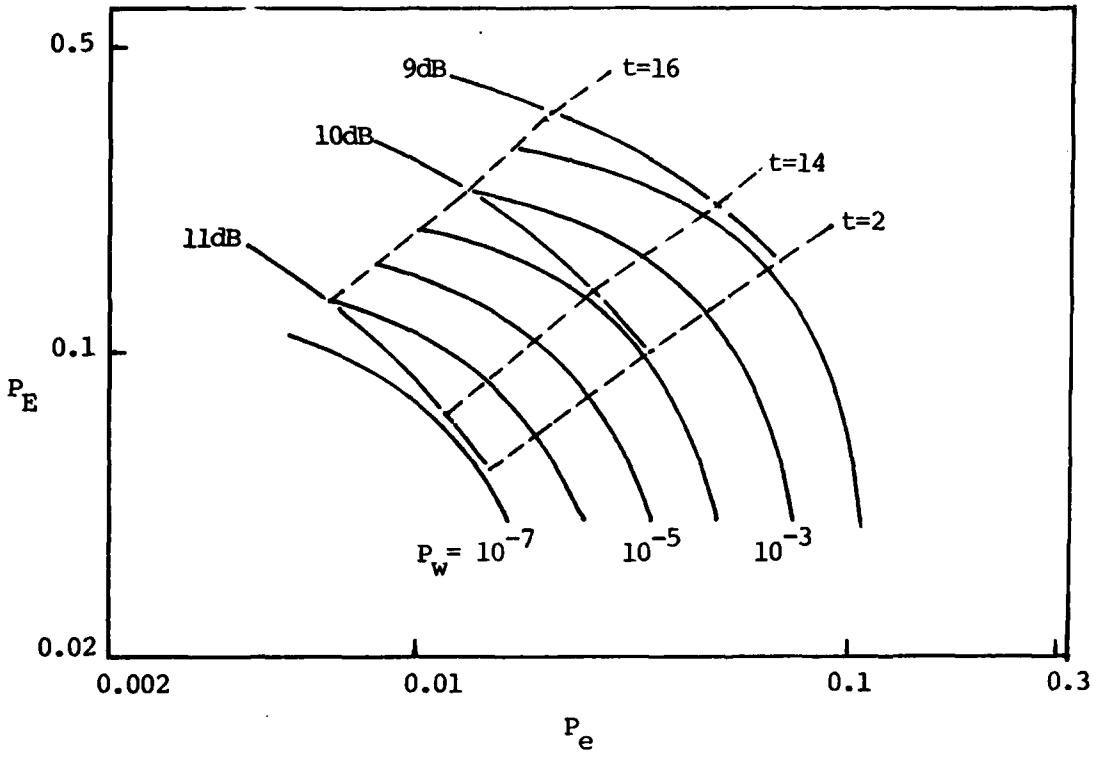

Figure 6.7. Monte Carlo simulation of digital correlation using the Welti codes.

The simulation results for the Welti codes agreed very well when compared to the simulation results for the modified maximal-length sequences. When the simulation results are compared with the results obtained from the performance analysis, we find that the simulation results deviated by an average of 0.5 dB.

6.3 Discussion of the Results of the Simulations

Monte Carlo simulation was used to verify the results obtained from the digital detection system analysis. The operation of a digital detection system using the threshold rule for its decision logic device was simulated. Two sets of orthogonal codes were investigated for possible variations in the performance results.

When the performance results of the Monte Carlo simulation using the maximal-length sequences are compared with the performance results of the Monte Carlo simulation using the Welti codes, the results agreed very well as expected for any orthogonal codes of length 32. The simulation results, however, were found to deviate from the results of the analysis by an average of 0.5 dB. Further investigation revealed that the deviation of the simulation results from the results of the analysis is due to a slight statistical correlation among the noise corrupted orthogonal codes. An in-depth analysis of the statistical behavior of the noise corrupted orthogonal codes is recommended for future research in this area.

CHAPTER 7

CONCLUSION

We started our investigation with the analog detection system. There we investigated the performance of the system which uses the threshold rule and the system which uses the ratio rule. The ratio rule was found to have an optimum ratio setting which was invariant with respect to changes in the SNR.

We next investigated the digital detection system. The threshold rule and the ratio rule were found to have the parameter setting which was invariant with respect to changes in the SNR. Compared to the performance of analog detection, the system performance for digital detection was worse by less than 1 dB.

Finally, Monte Carlo simulation of the digital detection system using the threshold rule was conducted. The results obtained from the Monte Carlo simulation using the maximal-length sequences agreed with the results obtained from the Monte Carlo simulation using the Welti codes. An average of Ø.5 dB deviation was found when the simulation results were compared with the results of the digital detection system performance analysis. An in-depth analysis of the statistical behavior of the noise-corrupted orthogonal codes is recommended for future research in this area.

REFERENCES

1. Macwilliams, F.J., Sloane, N.J.A., "The Theory of Error-Correcting Codes," North-Holland Publishing Company, Amsterdam, 1977, pp. 294-306.

2. Carlson, A. B., "Communication Systems," McGraw-Hill Book Company, New York, 1975, pp. 434-436.

3. Rosenstark, S. and Frank, J., "Investigation of Performance Degradation Due to Self-Jamming in Spread Spectrum Communications Systems," unpublished report, 1982.

4. Iverson, K. E., "A Programming Language," John Wiley and Sons, Inc., New York, 1962, p. 12.

5. Pasupathy, S., "Minimum Shift Keying: A Spectrally Efficient Modulation," IEEE Communications Magazine, July 1979, pp. 14-22.

6. Abramowitz, M. and Stegun, I., "Handbook of Mathematical Functions with Formulas, Graphs, and Mathematical Tables," U.S. Department of Commerce, National Bureau of Standards, Applied Mathematics Series 55, June 1964, p. 931.

7. Bhargava, Haccoun, Matyas, Nuspl, "Digital Communications by Satellite," John Wiley and Sons, Inc., New York, 1981, pp. 278-281.

8. Welti, G. R., "Quaternary Codes for Pulsed Radar," IRE Trans. Info. Th., June 1960, pp. 400-408.

ACKNOWLEDGMENT

The authors' understanding of the performance degradation due to self jamming in spread spectrum communications systems evolved to a large extent from discussions with Mr. Israel Mayk of the Center for Systems Engineering and Integration (CENSEI).

LIST OF ACRONYMS AND SYMBOLS

C^2	command and control
C^3	command, control, and communications
e	number of symbol errors
E	number of symbol erasures
E_c	peak chip-autocorrelation value
E_s	peak symbol-autocorrelation value
e_{min}	minimum value of e given S
e_{max}	maximum value of e given S
E_s/N_o	signal-to-noise ratio
FSK	frequency-shift keying
LFSRG	linear feedback shift-register generator
P_c	probability of a correct symbol
P_{ce}	probability of a chip error
P_e	probability of a symbol error
P_E	probability of a symbol erasure
P(k)	probability of k errors occurring in a 32-chip code word
P_w	probability of a word error
PSK	phase-shift keying
R-S	Reed-Solomon (code word)
S	a value which is equal to 2e plus E
SNR	signal-to-noise ratio

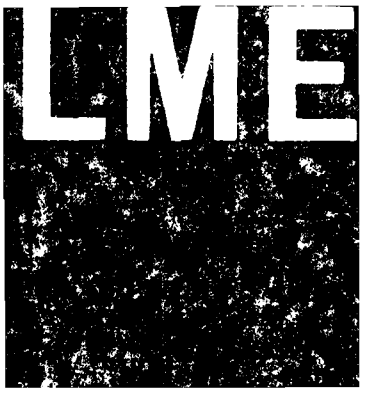
LME